

# Tunnelling Times in Quantum Mechanics

James Puleston

May 14, 2020

## **Abstract**

In this essay I survey recent developments in the theory of tunnelling times in quantum mechanics. The study of this concept is polarised depending on one's interpretation of quantum mechanics, which require different approaches and yield starkly different results. I survey this topic through the lenses of the orthodox (Copenhagen) and de Broglie-Bohm (pilot wave) interpretations, presenting the requisite theory and definitions and expounding the literature of the original authors through proofs and figures. I do this in sections 2 and 3 respectively. Before embarking on tunnelling times as a topic, I survey the conceptual aspects of how time is treated in classical and quantum mechanics. This topic has many subtle aspects which have hindered progress in understanding tunnelling times in the past. In this essay I hope to demonstrate the success that has been achieved in recent years, but also that further theoretical and experimental work is required, if we are to arrive at a universally accepted definition of tunnelling times in quantum mechanics - if indeed such a definition exists.

# Contents

<b>1</b>	<b>Introduction</b>	<b>4</b>
1.1	Time in Classical Mechanics . . . . .	4
1.2	Time in Quantum Mechanics . . . . .	5
<b>2</b>	<b>Tunnelling Times in the Orthodox Interpretation</b>	<b>7</b>
2.1	Tunnelling Through a Quantum Barrier . . . . .	7
2.2	Phase Times . . . . .	9
2.3	Dwell Time . . . . .	11
2.4	Continuous Cyclic Quantum Clock . . . . .	12
2.5	Discrete Cyclic Quantum Clock . . . . .	13
2.5.1	Application: Timing an Atomic Decay . . . . .	15
2.6	Larmor Precession . . . . .	17
2.6.1	The Strong-Field Limit . . . . .	19
2.6.2	Infinitesimal Field . . . . .	21
2.7	Summary . . . . .	24
<b>3</b>	<b>Tunnelling Times in the de Broglie-Bohm Interpretation</b>	<b>26</b>
3.1	de Broglie-Bohm Theory . . . . .	26
3.2	A Natural Definition of Tunnelling Time . . . . .	27
3.3	Numerical Example . . . . .	29
3.3.1	Parameters . . . . .	29
3.3.2	Crank-Nicolson Method . . . . .	29
3.3.3	de-Raedt Method . . . . .	31
3.4	A Crucial Experiment? . . . . .	32
<b>4</b>	<b>Conclusion</b>	<b>34</b>
<b>5</b>	<b>Acknowledgements</b>	<b>35</b>

# 1 Introduction

The treatment of time is one of the most important and open areas of research in the foundations of quantum mechanics. Time in the context of quantum tunnelling is a small yet divisive and diverse subset of this, the treatment of which differs drastically between adherents of the Copenhagen and pilot wave interpretations. To understand the wealth of different approaches to this subject, it is necessary to review the treatment of time in quantum mechanics as a whole. So in section 1.1 I outline its treatment in its predecessor theory, classical mechanics, and in section 1.2 describe how this evolves in to a quantum theory.

## 1.1 Time in Classical Mechanics

In the Hamiltonian formulation of classical mechanics, a system with  $n$  degrees of freedom possesses  $2n$  independent first-order differential equations in terms of  $2n$  independent variables. These variables are the coordinates of the *phase space* of the system, and the  $2n$  equations of motion describe the evolution of the system in the phase space.  $n$  of the independent variables are conventionally chosen to be the generalised coordinates  $q_i$  and the other  $n$  to be the conjugate momenta  $p_i$ , which obey the Poisson bracket relations (Goldstein 2002):

$$\{q_i, p_j\} = \delta_{ij} \quad \{q_i, q_j\} = \{p_i, p_j\} = 0, \quad i, j = \{1, \dots, n\}. \quad (1)$$

The time evolution of the canonical variables is governed by the Hamiltonian  $H = H(q_i, p_i)$ :

$$\frac{dq_i}{dt} = \{q_i, H\} \quad \frac{dp_i}{dt} = \{p_i, H\}. \quad (2)$$

For an infinitesimal variation in time,  $\delta t = \delta\tau$ , the associated variation in the dynamical variables is:

$$\delta q_i = \{q_i, H\}\delta\tau \quad \delta p_i = \{p_i, H\}\delta\tau. \quad (3)$$

$q_i$  and  $p_i$  are generalised variables; they are not necessarily positions and momenta, but in the case of a dynamical system comprised of a collection of point particles, the canonical variables are usually the particles' positions ( $\mathbf{q}_i$ ) and momenta ( $\mathbf{p}_i$ ).

In classical mechanics, physical systems are embedded in a 4-dimensional continuous space-time background, the points of which are assigned coordinates  $(t, x, y, z) = (t, \mathbf{x})$ . It is essential that the *definitions* of these two spaces and their associated coordinates are not conflated (Hilgevoord 2002). In particular we must distinguish the position variable  $\mathbf{q}$  from the space-time coordinate  $\mathbf{x}$ . The former defines a point in the phase space of the system (when accompanied by its associated momentum  $\mathbf{p}$ ) and is a property of a point particle, whereas the latter is the coordinate of a fixed point in the space-time background in which the dynamical system is embedded. Note that we can still introduce both sets of quantities in to equations and relate them, as equations (2) and (3) show.

Immediately this raises the question of whether there are physical systems that possess a dynamical variable that *resembles* the time coordinate of space-time. Such systems are called *clocks*: more precisely defined as physical systems with a dynamical 'clock' or 'time' variable that behaves similarly to the space-time time coordinate  $t$  under time translations. For example, under time translation in which the space-time coordinates transform as (cf. Hilgevoord 2002 (9), (10), (11)):

$$\mathbf{x} \rightarrow \mathbf{x} \quad t \rightarrow t + \tau \quad (4)$$

a *linear* clock variable  $\theta$  and its conjugate momentum  $\eta$  transform as:

$$\eta \rightarrow \eta \quad \theta \rightarrow \theta + \tau. \quad (5)$$

Comparing with (3) we see the infinitesimal case of (5):

$$\delta\eta = \{\eta, H\}\delta\tau \quad \delta\theta = \{\theta, H\}\delta\tau \quad (6)$$

which implies

$$\{\eta, H\} = 0 \quad \{\theta, H\} = 1. \quad (7)$$

The equation of motion given by (2),  $d\theta/dt = 1$  has solution  $\theta = t + t_0$ .

## 1.2 Time in Quantum Mechanics

In quantum mechanics the state of a particle is encoded in a vector  $|\psi\rangle$  in Hilbert space  $\mathcal{H}$ . Introducing a 1-dimensional continuum position basis in  $\mathcal{H}$ ,  $\{|q\rangle\}$ ,  $q \in \mathbb{R}$ , the state vector  $|\psi\rangle$  can be expanded as the integral (Sakurai 2017):

$$|\psi\rangle = \int_{\mathbb{R}} dq \psi(q) |q\rangle \quad (8)$$

where  $\psi(q)$  is the wave function of the particle. More generally, to describe a system in 3 dimensions requires a wave function  $\psi(q_x, q_y, q_z)$ . It is important to note that the domain of the wave function is the *configuration space* of the system,  $\mathbb{R}^3$ , whose coordinates are the generalised coordinates  $q_i$  of the system. It is common in elementary quantum mechanics literature for elements of the domain of the wave function to be expressed as  $(x, y, z)$ , i.e.  $\psi = \psi(x, y, z)$ . This is clearly in notational conflict with the use of  $(x, y, z)$  as coordinates of points of the background space-time in which the quantum system resides. In agreement with the literature surveyed in this essay I retain this notation throughout; but the distinction between space-time coordinates and dynamical variables should be maintained.

Measurable quantities or ‘observables’ are represented by operators on  $\mathcal{H}$ :

$$\mathcal{O} : \mathcal{H} \rightarrow \mathcal{H}. \quad (9)$$

Such operators arise through a procedure called ‘canonical quantisation’, which prescribes that *dynamical variables* of the Hamiltonian formalism are promoted to operators on  $\mathcal{H}$  and their Poisson bracket relations replaced by commutation relations according to:

$$\{\cdot, \cdot\} \rightarrow \frac{1}{i\hbar} [\cdot, \cdot]. \quad (10)$$

One notable omission in this process is the promotion of the time coordinate  $t$  to an operator. Given the emphasis placed on distinguishing between space-time coordinates and dynamical variables, the reason is clear: time  $t$  is a *space-time coordinate*, and canonical quantisation prescribes that *dynamical variables* are promoted to operators. However this raises the question of whether a time operator exists in quantum mechanics. The resolution of this problem has been historically hindered by a ‘proof’ offered by Wolfgang Pauli showing that the introduction of a time operator in quantum mechanics is forbidden. It proceeds roughly along the following lines (Butterfield 2012 section 4.3):

A Hermitian time operator  $T$ , which generates translations in  $H$  (the Hamiltonian) according to:

$$e^{i\tau T/\hbar} H e^{-i\tau T/\hbar} = H + \tau \mathbf{I} \quad \forall \tau \in \mathbb{R} \quad (11)$$

implies the spectrum of the Hamiltonian is  $\mathbb{R}$  because unitary transformations preserve the spectrum of an operator. Hence no Hermitian time operator can exist that is canonically conjugate to a general semibounded (from below) and discrete Hamiltonian.

Observing that this issue arose from erroneous attempts to quantise the *space-time* coordinate  $t$ , the problem becomes void: so that progress can be made by considering the quantisation of timelike *dynamical variables* of physical systems, namely clocks in analogy with the case in classical mechanics mentioned above.

Despite this clarification, approaches to the question *how long does a quantum particle take to tunnel through a classically forbidden potential barrier?* have not yielded a satisfactory answer that is universally agreed upon by the physics community. The question can be more formally posed as *when a particle with energy less than the barrier potential traverses the barrier region and is eventually transmitted, how much time did it, on average, spend in the barrier region?*

Overall, I argue that this topic has many subtle aspects arising as a consequence of the unique footing time is placed on in its treatment in quantum mechanics. Many solutions, reflecting these subtleties, have been offered to the question at hand within the orthodox interpretation. In section 2.1 I describe the physical

system (quantum tunnelling experiment) of interest, and in sections 2.2-2.6 I survey definitions within the orthodox viewpoint. However, the de Broglie-Bohm interpretation of quantum mechanics offers a clear and unambiguous answer to the question at hand. So in section 3.1 I introduce the requisite theory and in section 3.2 I present the natural definition of tunnelling time within the de Broglie-Bohm interpretation. In section 3.3 I report two numerical analyses of a quantum tunnelling experiment, and conclude in section 3.4 with a discussion of whether the drastic differences in predictions made by the rival interpretations can be exploited to break their long-standing empirical equivalence.

## 2 Tunnelling Times in the Orthodox Interpretation

In this section I survey a number of contenders for calculating the tunnelling time through a barrier. The definitions in sections 2.2-2.3 are ‘intrinsic’ quantities, in that they make no reference to a measuring apparatus (other than the implied particle detector to determine whether or not an incident particle is eventually transmitted) (Leavens 1996). Sections 2.4-2.5 propose models of a quantum clock, a physical system that when coupled to a system of interest can be used to measure time. Section 2.6 offers an ‘experimental’ definition, referring to a specific physical system.

Throughout this essay I use the physical system described in Büttiker (1983). The systems used in other literature surveyed in this essay differ by choice of coordinates and/or barrier location and I have accordingly recalculated various quantities, throughout the essay, for the physical system used by Büttiker and myself.

### 2.1 Tunnelling Through a Quantum Barrier

Consider the case of scattering in one dimension with particles of mass  $m$ , velocity  $v(k) = \hbar k/m$  and kinetic energy  $E = \hbar^2 k^2/2m$ . The particles move in the positive  $y$  direction and interact with a rectangular barrier, as shown in Figure 1:

$$V = \begin{cases} V_0 & -\frac{d}{2} < y < \frac{d}{2} \\ 0 & \text{otherwise} \end{cases} \quad (12)$$

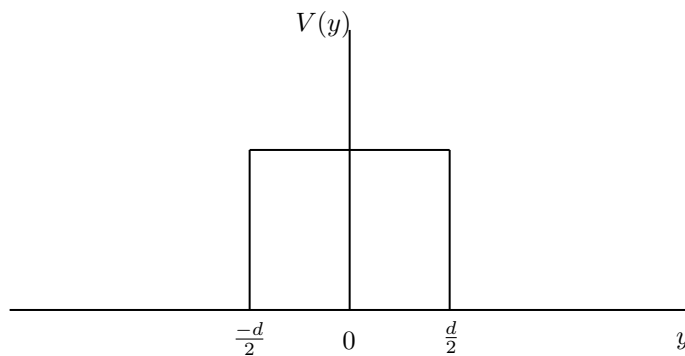


Figure 1: The quantum potential barrier

Note that  $E < V_0$  so that this system describes a quantum tunnelling experiment. The wave function is of the form:

$$\psi(y) = \begin{cases} e^{iky} + Ae^{-iky} & y \leq -\frac{d}{2} \\ Be^{\kappa y} + Ce^{-\kappa y} & -\frac{d}{2} \leq y \leq \frac{d}{2} \\ De^{iky} & y \geq \frac{d}{2} \end{cases} \quad (13)$$

where  $k = \sqrt{2mE}/\hbar$ ,  $\kappa := \sqrt{2m(V_0 - E)}/\hbar = \sqrt{k_0^2 - k^2}$  where  $k_0 = \sqrt{2mV_0}/\hbar$  and  $A, B, C, D$  are functions of the variables of the system.

The coefficient of the incident wave is set to one, corresponding to an average of one particle per unit length in the incident beam. Note there is no  $e^{-iky}$  term on the right of the barrier, as no particles are reflected after being transmitted through the barrier.

Calculation of the wave function coefficients  $A, B, C, D$  uses the continuity of the wave function and its first derivative at the barrier boundaries. The results are frequently stated without proof in the literature, but will be used so frequently in this essay that I provide a derivation. The results are:

$$\begin{aligned}
D &= T^{\frac{1}{2}} e^{i\Delta\phi} e^{-ikd} & A &= R^{\frac{1}{2}} e^{-i\pi/2} e^{i\Delta\phi} e^{-ikd} \\
B &= \frac{\kappa + ik}{2\kappa} e^{ikd/2} e^{-\kappa d/2} D & C &= \frac{\kappa - ik}{2\kappa} e^{ikd/2} e^{\kappa d/2} D
\end{aligned} \tag{14}$$

where  $T$  is the transmission probability,  $R = 1 - T$  is the reflection probability and  $\Delta\phi$  is the phase change across the barrier (calculated below) (Büttiker 1983).

*Proof.* First I introduce a new coordinate system so that the boundaries of the barrier become  $0, d$  i.e.  $\tilde{y} = y + d/2$ . Then, denoting the wave functions to the left of, inside, and to the right of the barrier as  $\psi_1, \psi_2, \psi_3$  respectively, yields:

$$\psi_1 = e^{-ikd/2} e^{ik\tilde{y}} + \tilde{A} e^{-ik\tilde{y}} \quad \psi'_1 = ik e^{ikd/2} e^{ik\tilde{y}} - ik \tilde{A} e^{-ik\tilde{y}} \tag{15a}$$

$$\psi_2 = \tilde{B} e^{\kappa\tilde{y}} + \tilde{C} e^{-\kappa\tilde{y}} \quad \psi'_2 = \kappa \tilde{B} e^{\kappa\tilde{y}} - \kappa \tilde{C} e^{-\kappa\tilde{y}} \tag{15b}$$

$$\psi_3 = \tilde{D} e^{ik\tilde{y}} \quad \psi'_3 = ik \tilde{D} e^{ik\tilde{y}} \tag{15c}$$

where  $\tilde{A} = A e^{ikd/2}$ ,  $\tilde{B} = B e^{-\kappa d/2}$ ,  $\tilde{C} = C e^{\kappa d/2}$ ,  $\tilde{D} = D e^{-ikd/2}$ .

Imposing continuity of the wave function and its first derivative at the barrier boundaries:

$$\psi_1(0) = \psi_2(0) \implies e^{-ikd/2} + \tilde{A} = \tilde{B} + \tilde{C} \tag{16a}$$

$$\psi'_1(0) = \psi'_2(0) \implies ik e^{-ikd/2} - ik \tilde{A} = \kappa \tilde{B} - \kappa \tilde{C} \tag{16b}$$

$$\psi_2(d) = \psi_3(d) \implies e^{\kappa d} \tilde{B} + e^{-\kappa d} \tilde{C} = e^{ikd} \tilde{D} \tag{16c}$$

$$\psi'_2(d) = \psi'_3(d) \implies \kappa e^{\kappa d} \tilde{B} - \kappa e^{-\kappa d} \tilde{C} = ik e^{ikd} \tilde{D} \tag{16d}$$

$$ik(16a) + (16b) \implies 2ike^{-ikd/2} = (ik + \kappa) \tilde{B} + (ik - \kappa) \tilde{C} \tag{16f}$$

$$\kappa(16c) + (16d) \implies 2\kappa e^{\kappa d} \tilde{B} = (\kappa + ik) e^{ikd} \tilde{D} \tag{16g}$$

$$\kappa(16c) - (16d) \implies 2\kappa e^{-\kappa d} \tilde{C} = (\kappa - ik) e^{ikd} \tilde{D}. \tag{16h}$$

Inserting equations (16g) and (16h) into equation (16f) one arrives at:

$$2ike^{-ikd/2} = -\frac{(ik - \kappa)^2}{2\kappa} e^{(ik+\kappa)d} \tilde{D} + \frac{(ik + \kappa)^2}{2\kappa} e^{(ik-\kappa)d} \tilde{D} \tag{17a}$$

$$\implies 4ik\kappa e^{-ikd} e^{-ikd/2} = \tilde{D} [(k^2 - \kappa^2)(e^{\kappa d} - e^{-\kappa d}) + 2ik\kappa(e^{\kappa d} + e^{-\kappa d})] \tag{17b}$$

$$= \tilde{D} [2(k^2 - \kappa^2) \sinh(\kappa d) + 4ik\kappa \cosh(\kappa d)]. \tag{17c}$$

Hence one arrives at the first result, the transmission probability  $T = |\tilde{D}|^2 (= |D|^2)$ :

$$T = \left[ 1 + \frac{(k^2 + \kappa^2)^2 \sinh^2(\kappa d)}{4k^2 \kappa^2} \right]^{-1}. \tag{18}$$

$\tilde{D}$  can be written in polar form:

$$\tilde{D} = |\tilde{D}| e^{i\theta} = T^{\frac{1}{2}} e^{i\theta} \tag{19a}$$

$$= \frac{2ik\kappa e^{-ikd} e^{-ikd/2} [(k^2 - \kappa^2) \sinh(\kappa d) - 2ik\kappa \cosh(\kappa d)]}{(k^2 - \kappa^2)^2 \sinh^2(\kappa d) + 4k^2 \kappa^2 \cosh^2(\kappa d)} \tag{19b}$$

$$\implies \theta = \arg(\tilde{D}) = \arctan \left( \frac{\text{Im}(\tilde{D})}{\text{Re}(\tilde{D})} \right) = -\frac{3kd}{2} + \arctan \left( \frac{k^2 - \kappa^2}{2k\kappa} \tanh(\kappa d) \right) \tag{19c}$$

where the first term comes from the exponential terms and the second term from the hyperbolic terms in (19b).

Using the form of  $\psi_3$  in (15), the *transmitted* wave function at  $\tilde{y} = d$  is:

$$\psi_3 = \tilde{D}e^{ikd} = T^{1/2}e^{i\theta}e^{ikd} \quad (20)$$

hence the phase at  $\tilde{y} = d$  is  $\theta + kd$ . Similarly using the form of  $\psi_1$ , the *incident* wave function at  $\tilde{y} = 0$  is:

$$\psi_1 = e^{-ikd/2} \quad (21)$$

hence the phase at  $\tilde{y} = 0$  is  $-kd/2$ . The phase change across the barrier is therefore:

$$\Delta\phi = \theta + \frac{3kd}{2} = -\frac{3kd}{2} + \arctan\left(\frac{k^2 - \kappa^2}{2k\kappa} \tanh(\kappa d)\right) + \frac{3kd}{2} = \arctan\left(\frac{k^2 - \kappa^2}{2k\kappa} \tanh(\kappa d)\right). \quad (22a)$$

Hence

$$\tilde{D} = T^{\frac{1}{2}}e^{i\Delta\phi}e^{-3ikd/2} \quad (23a)$$

$$D = T^{\frac{1}{2}}e^{i\Delta\phi}e^{-ikd} \quad (23b)$$

by substitution into equation 19a. The result for  $A$  follows along similar lines and results for  $B$  and  $C$  follow immediately from equations (16g) and (16h).  $\square$

## 2.2 Phase Times

Plane wave solutions to the quantum potential barrier (13), (14) are delocalised over all space. Superposition of plane waves with different momenta  $k$  yields waves which are localised in space, called wave packets. For example, one can construct a Gaussian wave packet from plane waves  $e^{iky}$ :

$$\psi(t, y) = \frac{1}{\sqrt{2\pi}} \int_{-\infty}^{\infty} dk \phi(k) e^{i(ky - w(k)t)} \quad w(k) = \frac{\hbar k^2}{2m} \quad (24a)$$

$$\phi(k) = \frac{1}{\sqrt{2\pi}} \int_{-\infty}^{\infty} dy \psi(0, y) e^{-iky} \quad \psi(0, y) = e^{-y^2 + ik_0 y} \quad (24b)$$

$$= \frac{1}{\sqrt{2}} e^{-(k - k_0)^2/4} \quad (24c)$$

where  $\psi(0, y)$  is the initial profile of the wave function and  $\phi(k)$  is the Fourier coefficient which is assumed to be sharply localised around  $k_0$ . The wave packet is shown in Figure 2.

In this instance the integral in (24a) can be accurately calculated by Taylor expansion of the dispersion relation around  $k_0$  to first order. However this will not necessarily work for other wave packets. To make progress, one can use the stationary phase approximation: given Fourier coefficient  $\phi(k)$  sharply localised around  $k = k_0$ , the integral (cf. (24a)) has non-zero value by dint of contributions from the integrand only in the region  $k \approx k_0$ , only if the plane wave term oscillates on scales larger than the region around  $k_0$  (the wave phase is ‘stationary’ in  $k$ -space).

Applying this method to the incident and transmitted plane waves in (13), (14) (accounting for time evolution under the time evolution operator  $U(t) = e^{-iEt/\hbar}$ ) yields:

$$\text{Incident:} \quad -\frac{1}{\hbar} \frac{dE}{dk} t + y_p(t) = 0 \quad (25a)$$

from which one derives the group velocity of the wave packet  $v_g = \hbar^{-1} dE/dk = \hbar k/m$ . This is the propagation velocity of the envelope wave and is identified with the particle velocity. This differs from the phase velocity  $v_p = w/k$  which is the propagation velocity of the carrier wave.

$$\text{Transmitted:} \quad \frac{d\Delta\phi}{dk} - \frac{1}{\hbar} \frac{dE}{dk} t + y_p(t) - d = 0 \quad (25b)$$

### Gaussian Wavepacket with Fourier coefficient

$$\phi(k) = \frac{e^{-\frac{1}{4}(k-k_0)^2}}{\sqrt{2}}, \quad t=0, \quad k_0=20, \quad m=1 \quad (\hbar=1)$$

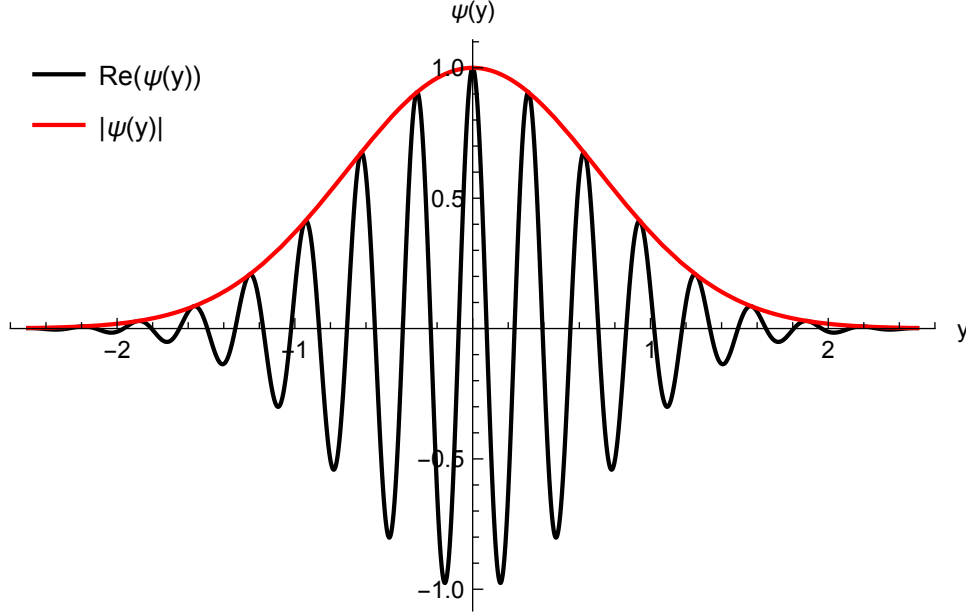


Figure 2: Gaussian wave packet (24a) showing the carrier wave (black) and amplitude modulating envelope wave (red). Produced by the author using Mathematica 12.0

(cf. Hauge and Støvneng 1989 (2.3)). Solving equations (25a) and (25b) for  $t$  at  $y_p(t) = -d/2$  and  $d/2$  respectively, one finds that the difference of these times, i.e. the traversal time of the peak across the barrier for the transmitted wave, is:

$$\tau_\phi = \hbar \frac{d\Delta\phi}{dE} = \frac{m}{\hbar k} \frac{d\Delta\phi}{dk} \quad (26)$$

(An identical result is obtained for a wave packet reflected from the barrier.) (cf. Büttiker 1983 (3.1)).

Equation (26) can be calculated explicitly using equation (22a):

$$\frac{m}{\hbar k} \frac{d\Delta\phi}{dk} = \frac{m}{\hbar k} \frac{d}{dk} \left( \arctan \left[ \frac{k^2 - \kappa^2}{2k\kappa} \tanh(\kappa d) \right] \right) \quad (27a)$$

$$= \frac{m}{\hbar k} \frac{1}{\left[ \frac{k^2 - \kappa^2}{2k\kappa} \tanh(\kappa d) \right]^2 + 1} \frac{1}{2} \frac{d}{dk} \left( \frac{k^2 - \kappa^2}{k\kappa} \tanh(\kappa d) \right). \quad (27b)$$

Recalling the relation between  $k$  and  $\kappa$  in (13), the derivative term evaluates to:

$$\left[ 2\kappa^{-1} + \frac{k^2}{\kappa^3} + \frac{\kappa}{k^2} \right] \tanh(\kappa d) + d \left( -\frac{k^2}{\kappa^2} + 1 \right) \text{sech}^2(\kappa d). \quad (27c)$$

Hence

$$\frac{m}{\hbar k} \frac{d\Delta\phi}{dk} = \frac{m}{2\hbar k} \frac{4k^2\kappa^2 \text{sech}^2(\kappa d)}{(k^2 - \kappa^2)^2 \tanh^2(\kappa d) + 4k^2\kappa^2} \left\{ \left[ 2\kappa^{-1} + \frac{k^2}{\kappa^3} + \frac{\kappa}{k^2} \right] \sinh(\kappa d) \cosh(\kappa d) - \frac{kd}{\kappa} \left( \frac{k}{\kappa} - \frac{\kappa}{k} \right) \right\} \quad (27d)$$

$$= \frac{2mk\kappa^2}{\hbar} \frac{1}{k_0^4 \sinh^2(\kappa d) + 4k^2\kappa^2} \left\{ \left[ 2\kappa^{-1} + \frac{k^2}{\kappa^3} + \frac{\kappa}{k^2} \right] \frac{\sinh(2\kappa d)}{2} - \frac{kd}{\kappa} \left( \frac{k}{\kappa} - \frac{\kappa}{k} \right) \right\}. \quad (27e)$$

The term in  $\{\dots\}$  is easily shown to be:

$$\{\dots\} = \frac{k_0^4}{k^2 \kappa^3} \frac{\sinh(2\kappa d)}{2} + \frac{d}{\kappa^2} (\kappa^2 - k^2) \text{ where } k_0^2 = k^2 + \kappa^2 \quad (27f)$$

yielding the final result:

$$\tau_\phi = \frac{m}{\hbar k \kappa} \frac{2k^2 \kappa d (\kappa^2 - k^2) + k_0^4 \sinh(2\kappa d)}{4k^2 \kappa^2 + k_0^4 \sinh^2(\kappa d)}. \quad (27g)$$

This is defined as the *phase-delay time* of the scattering process (cf. Büttiker 1983 (3.2)).

The same result is achieved via a different approach by Hauge and Støvneng (1989). They introduce an interval  $(y_1, y_2)$  containing the barrier (i.e.  $y_1 < -d/2, y_2 > d/2$ ) and using (25a) and (25b) they define (cf. Hauge and Støvneng 1989 (2.4)) the spatial *delay*  $\delta y_T$  as the change in phase induced by the barrier and the corresponding temporal delay  $\delta \tau_T$  for the transmitted wave packet:

$$\delta y_T = \frac{d\Delta\phi}{dk} - d \quad \delta \tau_T = \frac{1}{v(k)} \left[ \frac{d\Delta\phi}{dk} - d \right] \quad \text{where } v(k) = \frac{\hbar k}{m} \text{ is the group velocity;} \quad (28)$$

with analogous definitions for the reflected wave packet:

$$\delta y_R = d - \frac{d\Delta\phi}{dk} \quad \delta \tau_R = -\frac{1}{v(k)} \left[ d - \frac{d\Delta\phi}{dk} \right]. \quad (29)$$

They subsequently define (cf. Hauge and Støvneng 1989 (2.5, 2.6)) the total phase time for transmission:

$$\tau_T(y_1, y_2; k) = \frac{1}{v(k)} [y_2 - y_1 + \delta y_T] \quad (30)$$

and similarly the total phase time for reflection:

$$\tau_R(y_1, y_2; k) = \frac{1}{v(k)} [-2y_1 - \delta y_R] \quad (31)$$

where the minus sign before the spatial delay is picked up due to the wave packet travelling in the opposite direction.

By linearly extrapolating the interval  $(y_1, y_2) \rightarrow (-d/2, d/2)$ , one defines the *extrapolated phase times* (cf. Hauge and Støvneng 1989 (2.7, 2.8)):

$$\Delta\tau_T(-\frac{d}{2}, \frac{d}{2}; k) = \frac{1}{v(k)} [d + \delta y_T] \quad (32)$$

$$\Delta\tau_R(-\frac{d}{2}, \frac{d}{2}; k) = \frac{1}{v(k)} [d - \delta y_R]. \quad (33)$$

Substituting  $\delta y_T, \delta y_R$  in equations (28) and (29) into (32), (33) recovers (26) with  $\Delta\tau_T := \Delta\tau_T(-d/2, d/2; k) = \Delta\tau_R = \tau_\phi$ .

### 2.3 Dwell Time

The *dwell time*  $\tau_D$  is an expression for the average time spent by a particle in the barrier region, regardless of whether it is ultimately transmitted or reflected (Leavens and Aers 1990 pp. 59). Formally it is defined as the ratio of the average number of particles within the barrier region to the average number entering the barrier per unit time (quantified by the incident flux  $j$ ) (Büttiker 1983 (3.5)), (Leavens and Aers 1989 (1)):

$$\tau_D = \frac{\int_{-d/2}^{d/2} dy |\psi(t, y)|^2}{j(t, y)}. \quad (34)$$

Evaluating this quantity for the wave function inside the barrier region (13), (14) yields:

$$\psi = \frac{\kappa + ik}{2\kappa} T^{1/2} e^{i(\Delta\phi - kd/2)} e^{\kappa(y-d/2)} + \frac{\kappa - ik}{2\kappa} T^{1/2} e^{i(\Delta\phi - kd/2)} e^{-\kappa(y-d/2)} \quad (35a)$$

$$|\psi|^2 = \frac{\kappa^2 + k^2}{4\kappa^2} T \left( e^{\kappa(2y-d)} + e^{-\kappa(2y-d)} \right) + \frac{T}{4\kappa^2} \left( (\kappa + ik)^2 + (\kappa - ik)^2 \right) \quad (35b)$$

$$\int_{-d/2}^{d/2} dy |\psi(y)|^2 = \int_{-d/2}^{d/2} dy \frac{T}{4\kappa^2} \left[ (\kappa^2 + k^2) \left( e^{\kappa(2y-d)} + e^{-\kappa(2y-d)} \right) + (\kappa + ik)^2 + (\kappa - ik)^2 \right] \quad (35c)$$

$$= \int_{-d/2}^{d/2} dy \frac{T}{4\kappa^2} \left[ (\kappa^2 + k^2) 2 \cosh(\kappa(2y-d)) + 2(\kappa^2 - k^2) \right] \quad (35d)$$

$$= \frac{T}{4\kappa^2} \left[ \frac{k_0^2}{\kappa} \sinh(2\kappa d) + 2(\kappa^2 - k^2)d \right] \quad (35e)$$

then, using equation (18) for  $T$ :

$$= \frac{k^2}{\kappa} \frac{2\kappa d(\kappa^2 - k^2) + k_0^2 \sinh(2\kappa d)}{4k^2\kappa^2 + k_0^4 \sinh^2(\kappa d)} \quad (35f)$$

and for the incident flux with  $\psi(y) = e^{iky}$ :

$$j = -\frac{i\hbar}{2m} \left( \psi^* \frac{\partial \psi}{\partial y} - \psi \frac{\partial \psi^*}{\partial y} \right) \quad (35g)$$

$$= -\frac{i\hbar}{2m} (2ik) = \frac{\hbar k}{m} = v(k) \quad (35h)$$

so that (cf. Büttiker 1983 (3.6), (2.20b)):

$$\tau_D = \frac{1}{v(k)} \frac{k^2}{\kappa} \frac{2\kappa d(\kappa^2 - k^2) + k_0^2 \sinh(2\kappa d)}{4k^2\kappa^2 + k_0^4 \sinh^2(\kappa d)}. \quad (35i)$$

The phase times  $\tau_T$  and  $\tau_R$  represent conditional averages over mutually exclusive events (a particle cannot both reflect and transmit) (Hauge and Støvneng 1989 pp. 918). The dwell time  $\tau_D$  is the average over all scattering channels, and hence the conditional averages must obey the probabilistic rule:

$$\tau_D = T\tau_T + R\tau_R \quad (36)$$

where  $T$  and  $R = 1 - T$  are transmission and reflection probabilities respectively. Comparison of equations (27g) and (35i) show this consistency check is not satisfied:

$$\tau_T = \tau_R = \tau_\phi \implies T\tau_T + R\tau_R = \tau_\phi(T + R) = \tau_\phi \neq \tau_D. \quad (37)$$

Resolution of this issue comes from noticing that attaching *physical significance* to the time in (27g) is incorrect, as it requires the assumption that motion outside of the barrier is that of a free particle (Hauge and Støvneng (1989 pp. 924)). This is valid on the transmitted side of the barrier, however during approach to the barrier the incoming wave packet interferes with the reflected wave packet and hence motion can no longer be assumed to be free.

## 2.4 Continuous Cyclic Quantum Clock

In this section I present a theoretical model of a continuous cyclic quantum clock as provided by Hilgevoord (2002). This model acts as a precursor to the discrete cyclic quantum clock presented in section 2.5.

The angular variable  $\phi$  plays the role of the clock variable and is represented by the operator  $\hat{\Phi}$ . An angular momentum operator  $\hat{L}$  is also introduced and the two operators in the angular representation are given by (setting  $\hbar = 1$ ):

$$\hat{\Phi} = \phi \quad \hat{L} = -i \frac{d}{d\phi} \quad (38)$$

as is familiar from the theory of angular momentum in quantum mechanics. These operators act on a Hilbert space of square integrable functions of  $\phi$  with domain  $[0, 2\pi]$  as:

$$\hat{\Phi}f(\phi) = \phi f(\phi) \quad \hat{L}f(\phi) = -i \frac{d}{d\phi} f(\phi). \quad (39)$$

These operators have eigenvalue equations

$$\hat{\Phi}|\phi\rangle = \phi|\phi\rangle, \phi \in [0, 2\pi] \quad \hat{L}|m\rangle = m|m\rangle, m = 0, \pm 1, \pm 2, \dots \quad (40)$$

in which the eigenvectors form complete orthonormal sets such that:

$$\langle\phi|\phi'\rangle = \delta(\phi - \phi') \quad \langle m|m'\rangle = \delta_{mm'}. \quad (41)$$

Recalling from the theory of angular momentum in quantum mechanics that the  $\hat{L}_z = -i \frac{d}{d\phi}$  operator has eigenfunctions  $\propto e^{im\phi}$ ,  $|m\rangle$  has wave function  $\langle\phi|m\rangle = Ae^{im\phi}$  where  $A$  is calculated using the normalisation condition to be  $(2\pi)^{-\frac{1}{2}}$ :

$$u_m(\phi) := \langle\phi|m\rangle = (2\pi)^{-\frac{1}{2}} e^{im\phi}. \quad (42)$$

As  $\{|m\rangle\}$  form a complete set,  $|\phi\rangle$  can be expressed as:

$$|\phi\rangle = (2\pi)^{-\frac{1}{2}} \sum_{m=-\infty}^{\infty} e^{-im\phi} |m\rangle. \quad (43)$$

Introducing the Hamiltonian  $\hat{H} = \omega\hat{L}$ , the time evolution operator  $U(t) = e^{-iHt}$  acts as:

$$\hat{L}e^{-im\phi} |m\rangle = e^{-im\phi} \hat{L}|m\rangle \text{ by linearity of } \hat{L} \quad (44a)$$

$$= me^{-im\phi} |m\rangle; \quad (44b)$$

$$\implies e^{-iHt} |\phi\rangle = \sum_{n=0}^{\infty} \frac{(-i\omega t)^n}{n!} \hat{L}^n \left( (2\pi)^{-\frac{1}{2}} \sum_{m=-\infty}^{\infty} e^{-im\phi} |m\rangle \right) \quad (44c)$$

$$= (2\pi)^{-\frac{1}{2}} \sum_{n=0}^{\infty} \sum_{m=-\infty}^{\infty} \frac{(-i\omega m t)^n}{n!} e^{-im\phi} |m\rangle \quad (44d)$$

$$= (2\pi)^{-\frac{1}{2}} \sum_{m=-\infty}^{\infty} e^{-i\omega m t} e^{-im\phi} |m\rangle \quad (44e)$$

$$= |\phi + \omega t\rangle. \quad (44f)$$

by setting  $\omega = 1$ ,  $\phi$  plays exactly the same role as a time variable  $t$ .

## 2.5 Discrete Cyclic Quantum Clock

A discrete cyclic quantum clock can be modelled by limiting the sum in equation (43) to values of  $m$  satisfying  $-j \leq m \leq j$ , as presented by Peres (1980). The clock has an odd number  $N = 2j + 1$  of states represented by wave functions

$$u_m(\phi) = (2\pi)^{-\frac{1}{2}} e^{im\phi}, m = -j, \dots, j \text{ and } 0 \leq \phi \leq 2\pi. \quad (45)$$

One can construct an alternative orthogonal basis for the clock's wave functions

$$v_k(\phi) = N^{-\frac{1}{2}} \sum_{m=-j}^j e^{-2\pi i k m / N} u_m \quad (46a)$$

$$= (2\pi N)^{-\frac{1}{2}} \sum_{m=-j}^j [e^{i(\phi - 2\pi k / N)}]^m \quad \tilde{m} = m + j \quad (46b)$$

$$= (2\pi N)^{-\frac{1}{2}} \sum_{\tilde{m}=0}^{2j} [e^{i(\phi - 2\pi k / N)}]^{\tilde{m} - j} \quad (46c)$$

$$= (2\pi N)^{-\frac{1}{2}} [e^{i(\phi - 2\pi k / N)}]^{(1-N)/2} \sum_{\tilde{m}=0}^{2j} [e^{i(\phi - 2\pi k / N)}]^{\tilde{m}} \quad (46d)$$

$$= (2\pi N)^{-\frac{1}{2}} [e^{i(\phi - 2\pi k / N)}]^{(1-N)/2} \left( \frac{1 - (e^{i(\phi - 2\pi k / N)})^N}{1 - e^{i(\phi - 2\pi k / N)}} \right) \quad (46e)$$

$$= (2\pi N)^{-\frac{1}{2}} \frac{[e^{i(\phi - 2\pi k / N)}]^{1/2}}{1 - e^{i(\phi - 2\pi k / N)}} \left( (e^{i(\phi - 2\pi k / N)})^{-N/2} - (e^{i(\phi - 2\pi k / N)})^{N/2} \right) \quad (46f)$$

$$= (2\pi N)^{-\frac{1}{2}} \frac{\sin\left(\frac{N}{2}(\phi - 2\pi k / N)\right)}{\sin\left(\frac{1}{2}(\phi - 2\pi k / N)\right)} \quad \text{for } k = 0, \dots, N - 1. \quad (46g)$$

For large  $N$  these functions have a sharp peak at  $\phi = 2\pi k / N$  (see Figure 3), which we visualise as pointing to the  $k^{\text{th}}$  hour with angle uncertainty  $\pm\pi/N$ :

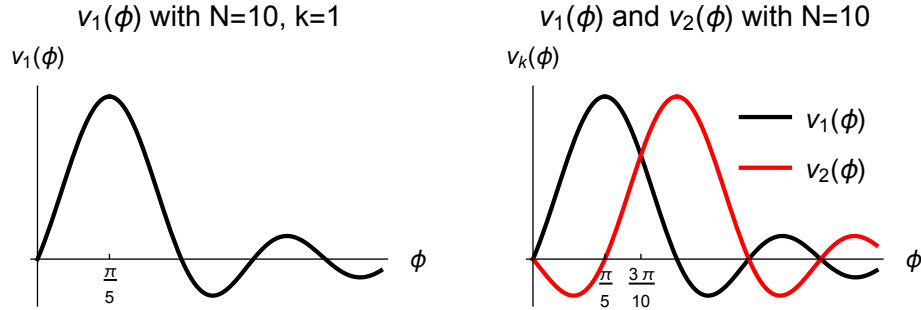


Figure 3: The wave functions of the discrete cyclic quantum clock are sharply peaked around  $\phi = 2\pi k / N$ . Produced by the author using Mathematica 12.0

One can then define projection operators  $P_k v_m = \delta_{km} v_m$  and a clock time operator  $T_c = \tau \sum k P_k$  where  $\tau$  is the resolution of the clock. The eigenvectors of  $T_c$  are  $v_k$  with eigenvalues  $t_k = k\tau, k = 0, \dots, N - 1$ . Hence measuring  $T_c$  yields discrete approximations to the true time, just as analog and digital clocks do.

The clock's Hamiltonian is:

$$H_c = \omega J \quad \text{where } \omega = \frac{2\pi}{N\tau} \quad \text{and } J = -i\hbar \frac{\partial}{\partial \phi} \quad (47)$$

The wave functions  $u_m$  are eigenfunctions of the Hamiltonian:

$$H_c u_m = m\hbar\omega u_m; \quad (48)$$

whence expanding the time evolution operator as a Taylor series gives:

$$e^{-iH_c t/\hbar} u_m = e^{-im\omega t} u_m = (2\pi)^{-\frac{1}{2}} e^{im(\phi - \omega t)} \quad (49a)$$

$$\implies e^{-iH_c \tau/\hbar} v_k = N^{-\frac{1}{2}} \sum_m e^{-2\pi i k m/N} e^{-2\pi i m/N} u_m \quad (49b)$$

$$= N^{-\frac{1}{2}} \sum_m e^{-2\pi i (k+1)m/N} u_m \quad (49c)$$

$$= v_{k+1}. \quad (49d)$$

where the equation for  $\omega$  in (47) has been used in (49b). Hence the clock passes successively through states  $v_0, v_1, \dots$  at time intervals  $\tau$ .

### 2.5.1 Application: Timing an Atomic Decay

One can apply the construction of the quantum clock to model timing an atomic decay (Peres 1980 section 4). The atom-clock system has Hamiltonian  $H = H_a + P_0 H_c$  where  $H_a$  is the Hamiltonian of the atom,  $H_c$  the Hamiltonian of the clock and  $P_0$  the projection operator for the atom's undecayed state. This coupling therefore represents the notion that the clock stops running when the atom decays.  $H_a$  is of the form  $H_a = H_0 + V$  where  $H_0$  has a continuous spectrum  $H_0 \phi(E) = E \phi(E)$   $E > E_{min}$ , plus one discrete eigenstate  $\phi_0$  with energy  $E_0 > E_{min}$ . All energy eigenstates are mutually orthogonal. The non vanishing matrix elements of  $V$  are denoted  $V(E) := \langle \phi(E) | V | \phi_0 \rangle$ , which is assumed to be almost constant in  $E$  over a large domain on both sides of  $E_0$ . In sum, one has:

$$H = H_a + P_0 H_c = H_0 + V + P_0 H_c. \quad (50)$$

The wave function for the atom can be expressed as:

$$\psi = a_0 \phi_0 e^{-iE_0 t/\hbar} + \int dE a(E) \phi(E) e^{-iEt/\hbar}. \quad (51)$$

Application of the Schrödinger equation for the atom yields:

$$i\hbar \dot{a}(E) = V(E) a_0 e^{i(E-E_0)t/\hbar}. \quad (52)$$

*Proof.*

$$|\psi\rangle = a_0 |\phi_0\rangle e^{-iE_0 t/\hbar} + \int dE a(E) |\phi(E)\rangle e^{-iEt/\hbar} \quad (53a)$$

$$\implies (H_0 + V) |\psi\rangle = a_0 E_0 |\phi_0\rangle e^{-iE_0 t/\hbar} + \int dE a(E) E |\phi(E)\rangle e^{-iEt/\hbar} \quad (53b)$$

$$\begin{aligned} &+ a_0 V |\phi_0\rangle e^{-iE_0 t/\hbar} + \int dE a(E) V |\phi(E)\rangle e^{-iEt/\hbar} \\ &= i\hbar \frac{d|\psi\rangle}{dt}. \end{aligned} \quad (53c)$$

Taking the inner product with  $\langle \phi(E') |$  on both sides and using the orthogonality conditions yields the final result.  $\square$

$a_0$  is given by the Weisskopf-Wigner ansatz, i.e.  $a_0 = e^{-\gamma t/\hbar}$ . Substitution into (52) and taking the limit as  $t \rightarrow \infty$  yields:

$$\lim_{t \rightarrow \infty} a(E) = \frac{V(E)}{E - E_0 + i\gamma} \quad (54)$$

and substituting this in to (51) yields

$$\lim_{t \rightarrow \infty} \psi(t) = \int dE \frac{V(E) \phi(E) e^{-iEt/\hbar}}{E - E_0 + i\gamma}. \quad (55)$$

Normalisation of the wave function implies:

$$\int dE \frac{|V(E)|^2}{(E - E_0)^2 + \gamma^2} = 1. \quad (56)$$

Using the identity:

$$\delta(E - E_0) = \frac{1}{\pi} \lim_{\gamma \rightarrow 0} \frac{\gamma}{(E - E_0)^2 + \gamma^2} \approx \frac{\gamma}{\pi} \frac{1}{(E - E_0)^2 + \gamma^2} \quad (57)$$

in (56) yields  $\gamma = \pi|V(E_0)|^2$ .

Coupling the atom to a clock using the clock Hamiltonian in (47):

$$H = H_a + P_0\omega J \quad (58)$$

and setting the initial state of the clock to  $v_0 = 1/\sqrt{N} \sum u_n$  as in (46a),  $J$  can be replaced by the numerical constant  $n\hbar$  by virtue of the eigenvalue equation (48). Note that this shifts the energy of the initial state  $E_0 \rightarrow E_0 + n\hbar\omega$ .

In the limit of large  $t$  the combined state of the atom and clock is:

$$\psi = N^{-\frac{1}{2}} \sum u_n \int dE \frac{V(E)\phi(E)e^{-iEt/\hbar}}{E - E_0 - n\hbar\omega + i\gamma}. \quad (59)$$

The density matrix representing the state of the clock is given by (Peres 1980 pp. 555):

$$\rho = Tr_a(|\psi\rangle\langle\psi|) = \frac{1}{N} \sum \frac{|u_n\rangle\langle u_m|}{1 + i\alpha(n - m)} \quad (60)$$

where  $Tr_a$  indicates the trace is to be taken over the atom degrees of freedom only, and  $\alpha = \hbar\omega/2\gamma$  is the angle through which the pointer turns during an average atom lifetime  $\hbar/2\gamma$ . From this the probability  $\langle P_k \rangle$  of finding the clock stopped at time  $t_k = k\tau \stackrel{(47)}{=} 2\pi k/N\omega$  is given by:

$$Tr(\rho P_k) = \frac{1}{N} \sum_{m,n} \frac{\langle v_k | u_n \rangle \langle u_m | v_k \rangle}{1 + i\alpha(n - m)} \quad (61a)$$

$$\stackrel{(46a)}{=} \frac{1}{N^2} \sum_{m,n=-j}^j \frac{e^{2\pi ik(n-m)/N}}{1 + i\alpha(n - m)}. \quad (61b)$$

The double summation can be evaluated as follows: Let  $p = n - m$  and  $q = n + m$ . The summation becomes:

$$Tr(\rho P_k) = \frac{1}{N^2} \sum_{p=-2j}^{2j} \sum_{q=q_1(p)}^{q_2(p)} \frac{e^{i\theta p}}{1 + i\alpha p} \quad (62)$$

where  $\theta = 2\pi k/N$ ,  $q_1$  and  $q_2$  are bounds that can be determined as follows:

For fixed  $p \in \{-2j, -2j + 1, \dots, 2j - 1, 2j\}$ , demonstrated by the dashed line in Figure 4, the upper and lower bounds can be read off to be:

$$q_1(p) = -2j + |p| \quad q_2(p) = 2j - |p| \quad (63)$$

Next noting that for fixed  $p$  of given parity, all  $q \in \{q_1(p), \dots, q_2(p)\}$  have the same parity and hence:

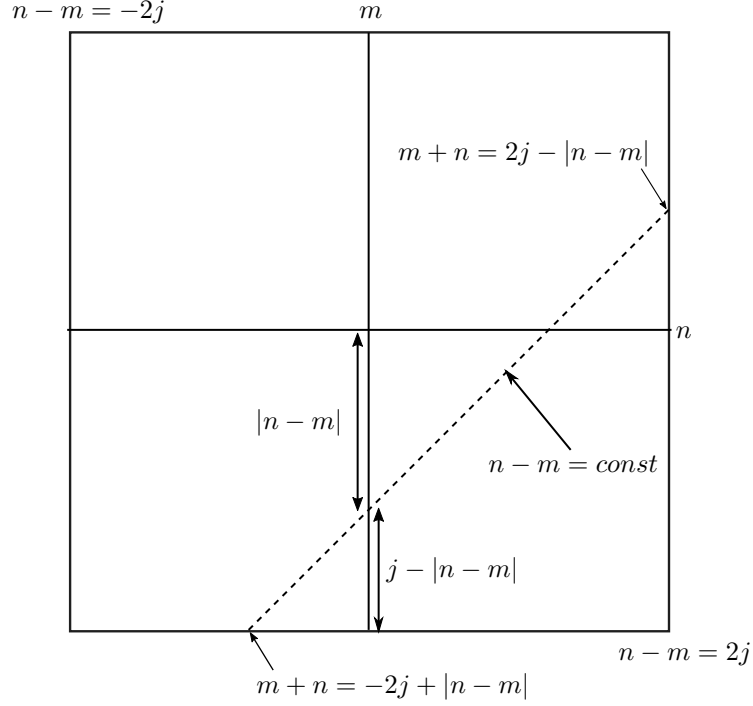


Figure 4: Bounds of the double sum in  $p, q$  coordinates

$$\text{Tr}(\rho P_k) = \frac{1}{N^2} \sum_{p=-2j}^{2j} \frac{e^{i\theta p}}{1 + i\alpha p} \sum_{q=-2j+|p|}^{2j-|p|} 1 \quad (64a)$$

$$= \frac{1}{N^2} \sum_{p=-2j}^{2j} \frac{e^{i\theta p}}{1 + i\alpha p} \left[ \frac{2j - |p| - (-2j + |p|)}{2} + 1 \right] \quad (64b)$$

$$= \frac{1}{N^2} \sum_{p=-2j}^{2j} \frac{(N - |p|)e^{i\theta p}}{1 + i\alpha p} \approx \frac{1}{N} \sum_{p=-2j}^{2j} \frac{e^{i\theta p}}{1 + i\alpha p} \quad (64c)$$

This result can be recognised as the Fourier series expansion of  $2\pi e^{-\theta/\alpha} / [N\alpha (1 - e^{-2\pi/\alpha})]$ ; and hence the clock stops (atoms decay) according to the exponential decay law, as expected.

## 2.6 Larmor Precession

In this section I consider the quantum barrier experiment as in section 2.1, but now with the additional constraints that the particles carry spin  $s = 1/2$  polarised in the x-direction, and with the presence of a small magnetic field  $\mathbf{B}_0$  parallel with the z-axis and confined to the width of the barrier (see Figure 5) (Büttiker 1983 section 1).

The magnetic field engenders on the particles in the barrier a Larmor precession of frequency  $\omega_L = g\mu B_0/\hbar$ , where  $g$  is the gyromagnetic ratio and  $\mu$  is the magnetic moment. This changes the spin of the particles to be polarised in the x-y plane such that (Rybachenko 1967):

$$\langle S_x \rangle \approx \frac{\hbar}{2} \quad \langle S_y \rangle \approx -\frac{\hbar}{2} \omega_L \tau_y. \quad (65)$$

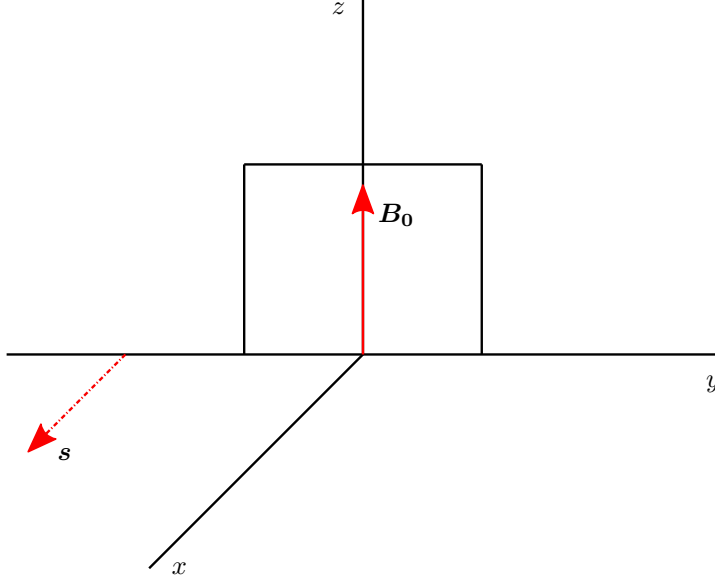


Figure 5: Experimental set up of a quantum barrier with a magnetic field constrained inside.

where  $\tau_y = \hbar k / V_0 \kappa$ . Rybachenko concludes that  $\tau_y$  is the time taken by the particle to traverse the barrier. However this analysis neglects consideration of the induced spin component aligned with the magnetic field: recall from the theory of spin in quantum mechanics that particles with spin in the x-direction can be represented as a linear combination of particles with spin in the  $\pm z$  directions:

$$|x; \pm\rangle = \frac{1}{\sqrt{2}} |z; +\rangle \pm \frac{1}{\sqrt{2}} |z; -\rangle \quad (66)$$

with z-components  $\pm\hbar/2$  each with probability 0.5. Inside the barrier the magnetic field induces a Zeeman shift  $\pm\hbar\omega_L/2$  to the energies of the particles, giving rise to different exponential decays of the wave functions inside the barrier (13)<sup>1</sup> (cf. Büttiker 1983 (1.5)):

$$\kappa_{\pm} = \left(k_0^2 - k^2 \mp \frac{m\omega_L}{\hbar}\right)^{\frac{1}{2}} \quad (67)$$

where  $\kappa_+$  ( $\kappa_-$ ) corresponds to particles with spin z parallel (antiparallel) to the magnetic field. In the limit  $\mathbf{B}_0 \propto \omega_L$  is small,  $\kappa_{\pm}$  can be approximated as:

$$\kappa_{\pm} = \left(k_0^2 - k^2 \mp \frac{m\omega_L}{\hbar}\right)^{\frac{1}{2}} \quad (68a)$$

$$= \kappa \left(1 \mp \frac{m\omega_L}{\hbar\kappa^2}\right)^{\frac{1}{2}} \quad (68b)$$

$$\approx \kappa \left(1 \mp \frac{m\omega_L}{2\hbar\kappa^2}\right) \quad (68c)$$

$$= \kappa \mp \frac{m\omega_L}{2\hbar\kappa}. \quad (68d)$$

As  $\kappa_+ < \kappa_-$ , particles with spin aligned with the magnetic field penetrate more easily than particles with

<sup>1</sup>Note I ignore the exponentially growing term in (13) because it is multiplied by a suppressive pre-factor  $e^{-\kappa d/2}$  in equation (14).

spin anti-aligned with the field, reflected in the transmission probability (cf. Büttiker 1983 (1.7)):

$$T \stackrel{(18)}{=} \left[ 1 + \frac{(k^2 + \kappa^2)^2 \sinh^2 \kappa d}{4k^2 \kappa^2} \right]^{-1} \quad (69a)$$

$$\approx \left[ \frac{(k^2 + \kappa^2)^2 e^{2\kappa d}}{4k^2 \kappa^2 4} \right]^{-1} \quad (69b)$$

$$= \frac{16k^2 \kappa^2}{(k^2 + \kappa^2)^2} e^{-2\kappa d} \quad (69c)$$

$$\implies T_{\pm} = T e^{\pm \omega_L \tau_z} \quad (69d)$$

where  $\tau_z = md/\hbar\kappa$  is the time a particle with velocity  $v(k) = \hbar k/m$  takes to traverse the barrier (the subscript ‘z’ is chosen because the quantity arises in the spin-z expectation value (70), and does not denote the propagation ( $y$ ) direction). The approximation to  $T$  assumes the limit of an opaque barrier,  $k_0 d \gg 1$ . Hence the barrier with the magnetic field induces a net  $z$ -component of spin polarisation aligned with the field, quantified by the ratio of excess flux to total flux:

$$\langle S_z \rangle = \frac{\hbar T_+ - T_-}{2 T_+ + T_-} = \frac{\hbar}{2} \tanh \omega_L \tau_z. \quad (70)$$

The polarisation of the transmitted and reflected particles for all incident energies can be calculated. To do so one must solve the scattering problem with the Hamiltonian (cf. Büttiker 1983 (2.1)):

$$H = \begin{cases} \left( \frac{p^2}{2m} + V_0 \right) \mathbb{1} - \left( \frac{\hbar \omega_L}{2} \right) \sigma_z & |y| \leq \frac{d}{2} \\ \left( \frac{p^2}{2m} \right) \mathbb{1} & |y| \geq \frac{d}{2} \end{cases} \quad (71)$$

where  $\mathbb{1}$  is the  $2 \times 2$  identity matrix and  $\sigma_x, \sigma_y, \sigma_z$  are the Pauli spin matrices.  $H$  acts on spinors

$$\psi = \begin{pmatrix} \psi_+(y) \\ \psi_-(y) \end{pmatrix}. \quad (72)$$

As usual  $|\psi_{\pm}(y)|^2 dy$  is the probability of finding a particle *upon measurement* with spin  $\pm \hbar/2$  in the interval  $y, y + dy$ . I emphasise ‘upon measurement’ here as this is an important point of distinction between the orthodox and pilot wave interpretations addressed in this essay. The incident beam is polarised in the  $x$ -direction:

$$\psi = \frac{1}{\sqrt{2}} \begin{pmatrix} 1 \\ 1 \end{pmatrix} e^{iky} \quad (73)$$

i.e.  $\psi$  is an eigenvector of  $S_x$ .

$H$  is diagonal in the spinor basis so one can solve the scattering problem for particles with spin  $\hbar/2$  and  $-\hbar/2$  separately. This amounts to solving the quantum barrier in (13) with the following adjustments:

For particles with spin aligned(anti-aligned) with the magnetic field:

- $\kappa \rightarrow \kappa_+(\kappa_-)$
- $V_0 \rightarrow V_0 + (-)\frac{\hbar \omega_L}{2}$
- $A, B, C, D$  in (14)  $\rightarrow A_{+(-)}, B_{+(-)}, C_{+(-)}, D_{+(-)}$  by replacing  $\kappa \rightarrow \kappa_+(\kappa_-)$ .

### 2.6.1 The Strong-Field Limit

The transmitted particles have spinor:

$$\psi_T = (|D_+|^2 + |D_-|^2) \begin{pmatrix} D_+ \\ D_- \end{pmatrix}. \quad (74)$$

Recalling the Pauli sigma matrices:

$$\sigma_x = \begin{pmatrix} 0 & 1 \\ 1 & 0 \end{pmatrix} \quad \sigma_y = \begin{pmatrix} 0 & -i \\ i & 0 \end{pmatrix} \quad \sigma_z = \begin{pmatrix} 1 & 0 \\ 0 & -1 \end{pmatrix} \quad (75)$$

one finds for the expectation values of spin for the transmitted particles (cf. Büttiker 1983 (2.11)):

$$\langle S_z \rangle_T = \frac{\hbar}{2} \langle \psi_T | \sigma_z | \psi_T \rangle = \frac{\hbar}{2} \frac{|D_+|^2 - |D_-|^2}{|D_+|^2 + |D_-|^2} \quad (76a)$$

$$\langle S_y \rangle_T = \frac{\hbar}{2} \langle \psi_T | \sigma_y | \psi_T \rangle = i \frac{\hbar}{2} \frac{D_+ D_-^* - D_+^* D_-}{|D_+|^2 + |D_-|^2} \quad (76b)$$

$$\langle S_x \rangle_T = \frac{\hbar}{2} \langle \psi_T | \sigma_x | \psi_T \rangle = \frac{\hbar}{2} \frac{D_+ D_-^* + D_+^* D_-}{|D_+|^2 + |D_-|^2}. \quad (76c)$$

Using (14) and the adjustments for the magnetic field outlined above, one finds (cf. Büttiker 1983 (2.12a-c)):

$$\langle S_z \rangle_T = \frac{\hbar}{2} \frac{T_+ - T_-}{T_+ + T_-}. \quad (77)$$

*Proof.* Follows immediately from the fact that  $T = |D|^2$ .  $\square$

$$\langle S_y \rangle_T = -\hbar \sin(\Delta\phi_+ - \Delta\phi_-) \frac{(T_+ T_-)^{\frac{1}{2}}}{T_+ + T_-}. \quad (78)$$

*Proof.*

$$\langle S_y \rangle_T = i \frac{\hbar}{2} \left( \frac{(T_+ T_-)^{\frac{1}{2}}}{T_+ + T_-} \right) \left( e^{i(\Delta\phi_+ - \Delta\phi_-)} - e^{-i(\Delta\phi_+ - \Delta\phi_-)} \right) \quad (79a)$$

$$= i \frac{\hbar}{2} \left( \frac{(T_+ T_-)^{\frac{1}{2}}}{T_+ + T_-} \right) (2i \sin(\Delta\phi_+ - \Delta\phi_-)) \quad (79b)$$

$$= -\hbar \sin(\Delta\phi_+ - \Delta\phi_-) \frac{(T_+ T_-)^{\frac{1}{2}}}{T_+ + T_-}. \quad (79c)$$

$\square$

$$\langle S_x \rangle_T = \hbar \cos(\Delta\phi_+ - \Delta\phi_-) \frac{(T_+ T_-)^{\frac{1}{2}}}{T_+ + T_-} \quad (80)$$

follows along similar lines to the case of  $\langle S_y \rangle_T$ .

These derivations have used no assumptions about the strength of the field, and so they hold for arbitrary magnetic field. Using the approximation to  $T$  in (69) one sees that  $T_+ \propto e^{-2\kappa_+ d}$  and  $T_- \propto e^{-2\kappa_- d}$ . As  $\kappa_- > \kappa_+$ , for a sufficiently opaque barrier ( $k_0 d \gg 1$ ),  $T_+ \gg T_-$ , and therefore:

$$\langle S_z \rangle_T \approx \frac{\hbar}{2} \quad \langle S_y \rangle_T = \langle S_x \rangle_T \approx 0. \quad (81)$$

Hence the transmitted beam is almost exclusively polarised parallel to the magnetic field.

By similar arguments, with the spinor:

$$\psi_R = (|A_+|^2 + |A_-|^2) \begin{pmatrix} A_+ \\ A_- \end{pmatrix} \quad (82)$$

one arrives at the analogous results for the reflected wave (cf. Büttiker 1983 (2.14)):

$$\langle S_z \rangle_R = \frac{\hbar}{2} \frac{R_+ - R_-}{R_+ + R_-} \quad (83a)$$

$$\langle S_y \rangle_R = -\hbar \sin(\Delta\phi_+ - \Delta\phi_-) \frac{(R_+ R_-)^{\frac{1}{2}}}{R_+ + R_-} \quad (83b)$$

$$\langle S_x \rangle_R = \hbar \cos(\Delta\phi_+ - \Delta\phi_-) \frac{(R_+ R_-)^{\frac{1}{2}}}{R_+ + R_-}. \quad (83c)$$

Using the statement of particle conservation  $R_+ - R_- = -(T_+ - T_-)$ , one finds that:

$$\langle S_z \rangle_R = -\langle S_z \rangle_T \frac{T_+ + T_-}{R_+ + R_-} \quad (84a)$$

$$\langle S_y \rangle_R = \langle S_y \rangle_T \left( \frac{R_+ R_-}{T_+ T_-} \right)^{\frac{1}{2}} \frac{T_+ + T_-}{R_+ + R_-} \quad (84b)$$

$$\langle S_x \rangle_R = \langle S_x \rangle_T \left( \frac{R_+ R_-}{T_+ T_-} \right)^{\frac{1}{2}} \frac{T_+ + T_-}{R_+ + R_-} \quad (84c)$$

and hence  $\langle S_z \rangle_R + \langle S_z \rangle_T = 0$ , the statement of conservation of angular momentum.

## 2.6.2 Infinitesimal Field

In this section I report the study of polarisation of the transmitted and reflected waves in the limit of an infinitesimal field. Using (68d), one finds the result (cf. Büttiker 1983 (2.16)):

$$T_+ - T_- = T(\kappa_+) - T(\kappa_-) \quad (85a)$$

$$= \frac{T(k - m\omega_L/2\hbar\kappa) - T(k + m\omega_L/2\hbar\kappa)}{m\omega_L/\hbar\kappa} \times \frac{m\omega_L}{\hbar\kappa} \quad (85b)$$

$$\approx -\left( \frac{m\omega_L}{\hbar\kappa} \right) \frac{\partial T}{\partial \kappa}. \quad (85c)$$

In equation (85c) the Larmor frequency  $\omega_L$  is multiplied by a time  $(m/\hbar\kappa)\partial T/\partial \kappa$ . This motivates the definition of the characteristic times  $\tau_{zT}, \tau_{yT}, \tau_{xT}$  such that:

$$\langle S_z \rangle_T = \frac{\hbar}{2} \omega_L \tau_{zT} \quad (86a)$$

$$\langle S_y \rangle_T = -\frac{\hbar}{2} \omega_L \tau_{yT} \quad (86b)$$

$$\langle S_x \rangle_T = \frac{\hbar}{2} \left( 1 - \frac{\omega_L^2 \tau_{xT}^2}{2} \right). \quad (86c)$$

Using equations (77), (78) and (80) and the approximation  $T_+ + T_- \approx 2T$ , one can derive explicit results for the characteristic times (cf. Büttiker 1983 (2.18a-c)):

$$\tau_{zT} = -\left( \frac{m}{\hbar\kappa} \right) \frac{\partial \ln T^{\frac{1}{2}}}{\partial \kappa}. \quad (87)$$

*Proof.*

$$\langle S_z \rangle_T \stackrel{(77)}{=} \frac{\hbar T_+ - T_-}{2 T_+ + T_-} \quad (88a)$$

$$\approx \frac{\hbar T_+ - T_-}{4 T} \quad (88b)$$

$$\stackrel{(85c)}{=} -\frac{m\omega_L}{\hbar\kappa} \frac{\hbar}{4 T} \frac{\partial T}{\partial \kappa} \quad (88c)$$

$$= -\frac{m\omega_L}{\hbar\kappa} \frac{\hbar}{2} \frac{\partial \ln T^{\frac{1}{2}}}{d\kappa} \quad (88d)$$

$$= \frac{\hbar}{2} \omega_L \tau_{zT}. \quad (88e)$$

□

$$\tau_{yT} = -\left(\frac{m}{\hbar\kappa}\right) \frac{\partial \Delta\phi}{\partial \kappa}. \quad (89)$$

*Proof.*

$$\langle S_y \rangle_T \stackrel{(78)}{=} -\hbar \sin(\Delta\phi_+ - \Delta\phi_-) \frac{(T_+ T_-)^{\frac{1}{2}}}{T_+ + T_-} \quad (90a)$$

$$\sin(\Delta\phi_+ - \Delta\phi_-) \approx \Delta\phi_+ - \Delta\phi_- \approx \Delta(\Delta\phi) \text{ where } \Delta\phi := \phi_+ - \phi_- \quad (90b)$$

$$\implies \langle S_y \rangle_T \approx -\frac{\hbar}{2} \Delta(\Delta\phi) \text{ as } \frac{(T_+ T_-)^{\frac{1}{2}}}{T_+ + T_-} \approx \frac{1}{2} \quad (90c)$$

$$\Delta\kappa := \kappa_+ - \kappa_- = -\frac{m\omega_L}{\hbar\kappa} \quad (90d)$$

$$\implies \langle S_y \rangle_T = -\frac{\hbar}{2} \frac{\Delta(\Delta\phi)}{\Delta\kappa} \Delta\kappa \quad (90e)$$

$$\approx -\frac{\hbar}{2} \frac{\partial \Delta\phi}{\partial \kappa} \left(-\frac{m\omega_L}{\hbar\kappa}\right) \quad (90f)$$

$$= -\frac{\hbar}{2} \omega_L \tau_{yT}. \quad (90g)$$

□

$$\tau_{xT} = \left(\frac{m}{\hbar\kappa}\right) \left[ \left(\frac{\partial \Delta\phi}{\partial \kappa}\right)^2 + \left(\frac{\partial \ln T^{\frac{1}{2}}}{\partial \kappa}\right)^2 \right]^{\frac{1}{2}} \quad (91a)$$

$$= \left(\frac{m}{\hbar\kappa}\right) \left| D^{-1} \frac{\partial D}{\partial \kappa} \right|. \quad (91b)$$

*Proof.* Equation (91a) can be proven using similar methods to above but can be proven more easily by noting that since  $\langle S_x \rangle^2 + \langle S_y \rangle^2 + \langle S_z \rangle^2 = \frac{\hbar^2}{4}$  then  $\tau_{xT} = (\tau_{yT}^2 + \tau_{zT}^2)^{\frac{1}{2}}$ . Equation (91b) follows simply using the form of  $D$  in (14). □

The derivatives in (87), (89) can be evaluated explicitly to give:

$$\tau_{zT} = \frac{mk_0^2 (\kappa^2 - k^2) \sinh^2(\kappa d) + (\kappa dk_0^2/2) \sinh(2\kappa d)}{\hbar\kappa^2 (4k^2\kappa^2 + k_0^4 \sinh^2(\kappa d))}. \quad (92)$$

*Proof.*

$$\tau_{zT} \stackrel{(87)}{=} - \left( \frac{m}{\hbar\kappa} \right) \frac{\partial \ln T^{\frac{1}{2}}}{\partial \kappa} \quad (93a)$$

$$= \frac{m}{2\hbar\kappa} \frac{\partial}{\partial \kappa} \ln \left[ 1 + \frac{(k^2 + \kappa^2)^2 \sinh^2(\kappa d)}{4k^2\kappa^2} \right] \quad (93b)$$

$$= \frac{m}{2\hbar\kappa} \left[ 1 + \frac{k_0^4 \sinh^2(\kappa d)}{4k^2\kappa^2} \right]^{-1} \frac{1}{4k^2} \frac{\partial}{\partial \kappa} \left[ \frac{k_0^4 \sinh^2(\kappa d)}{\kappa^2} \right] \quad (93c)$$

the derivative term evaluates to:

$$\frac{\partial}{\partial \kappa} [\dots] = 2 \left( -\frac{k^4}{\kappa^3} + \kappa \right) \sinh^2(\kappa d) + \left( \frac{k^4}{\kappa^2} + 2k^2 + \kappa^2 \right) d \sinh(2\kappa d) \quad (93d)$$

$$\Rightarrow \tau_{zT} = \frac{m}{2\hbar} \frac{\kappa}{4k^2\kappa^2 + k_0^4 \sinh^2(\kappa d)} \left[ 2 \frac{\kappa^4 - k^4}{\kappa^3} \sinh^2(\kappa d) + \frac{k^4\kappa + 2k^2\kappa^3 + \kappa^5}{\kappa^3} d \sinh(2\kappa d) \right] \quad (93e)$$

$$= \frac{m}{\hbar\kappa^2} \frac{1}{4k^2\kappa^2 + k_0^4 \sinh^2(\kappa d)} \left[ (\kappa^2 - k^2)k_0^2 \sinh^2(\kappa d) + \frac{1}{2}k_0^4\kappa d \sinh(2\kappa d) \right] \quad (93f)$$

$$= \frac{mk_0^2}{\hbar\kappa^2} \frac{(\kappa^2 - k^2) \sinh^2(\kappa d) + (\kappa dk_0^2/2) \sinh(2\kappa d)}{4k^2\kappa^2 + k_0^4 \sinh^2(\kappa d)}. \quad (93g)$$

□

$$\tau_{yT} = \frac{mk}{\hbar\kappa} \frac{2\kappa d(\kappa^2 - k^2) + k_0^2 \sinh(2\kappa d)}{4k^2\kappa^2 + k_0^4 \sinh^2(\kappa d)}. \quad (94)$$

*Proof.*

$$\tau_{yT} \stackrel{(89)}{=} - \left( \frac{m}{\hbar\kappa} \right) \frac{\partial \Delta\phi}{\partial \kappa} \quad (95a)$$

$$= - \frac{m}{\hbar\kappa} \frac{1}{1 + \left( \frac{k^2 - \kappa^2}{2k\kappa} \tanh(\kappa d) \right)^2} \frac{\partial}{\partial \kappa} \left[ \left( \frac{k}{2\kappa} - \frac{\kappa}{2k} \right) \tanh(\kappa d) \right] \quad (95b)$$

$$= - \frac{m}{\hbar\kappa} \frac{4k^2\kappa^2}{4k^2\kappa^2 + (k^2 - \kappa^2)^2 \tanh^2(\kappa d)} \left[ - \left( \frac{k}{2\kappa^2} + \frac{1}{2k} \right) \tanh(\kappa d) + \left( \frac{k}{2\kappa} - \frac{\kappa}{2k} \right) d \operatorname{sech}^2(\kappa d) \right] \quad (95c)$$

$$= \frac{mk}{\hbar\kappa} \frac{2\kappa d(\kappa^2 - k^2) + k_0^2 \sinh(2\kappa d)}{4k^2\kappa^2 + k_0^4 \sinh^2(\kappa d)}. \quad (95d)$$

□

Note in taking  $\partial\Delta\phi/\partial\kappa$ , one assumes  $k$  and  $\kappa$  are no longer related by the equation in (13) such that taking the derivative with respect to  $\kappa$  whilst keeping  $k$  constant makes sense. The dependence of these characteristic times on wavenumber is shown in Figure 6.

One can define characteristic reflection times  $\tau_{zR}, \tau_{yR}, \tau_{xR}$  analogous to those in (86) such that:

$$\langle S_z \rangle_R = \frac{\hbar}{2} \omega_L \tau_{zR} \quad (96a)$$

$$\langle S_y \rangle_R = -\frac{\hbar}{2} \omega_L \tau_{yR} \quad (96b)$$

$$\langle S_x \rangle_R = \frac{\hbar}{2} \left( 1 - \frac{\omega_L^2 \tau_{xR}^2}{2} \right) \quad (96c)$$

By application of equations (84), one arrives at:

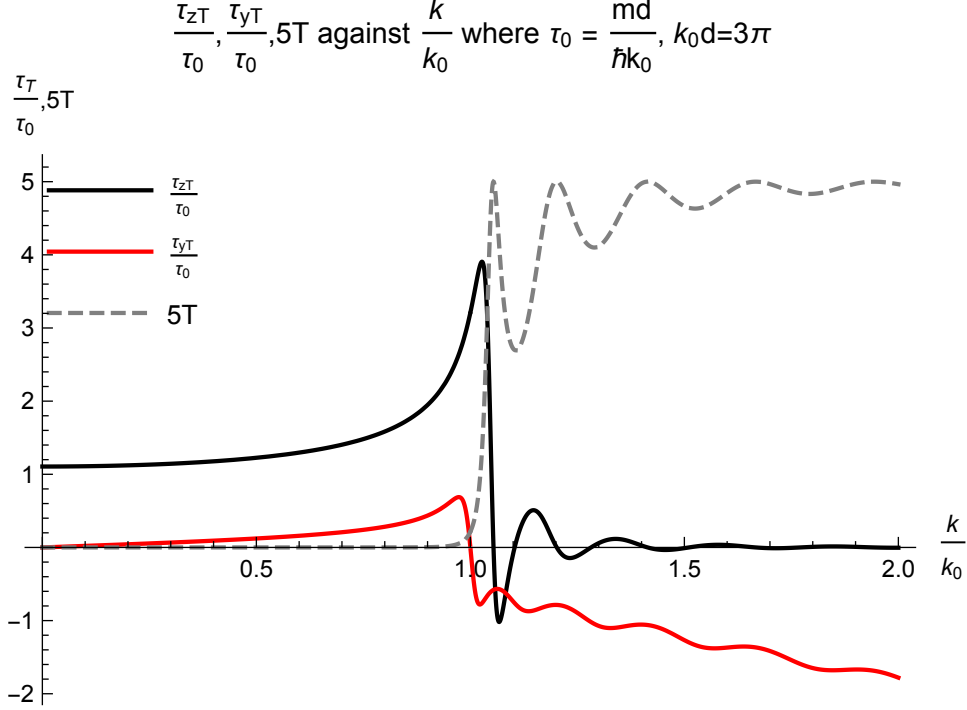


Figure 6: Dependence of the characteristic transmission times and transmission probability on wavenumber. Produced by the author using Mathematica 12.0

$$\tau_{zR} = -\tau_{zT} \frac{T}{R} \quad (97a)$$

$$\tau_{yR} = \tau_{yT} \quad (97b)$$

$$\tau_{xR} = (\tau_{yR}^2 + \tau_{zR}^2)^{\frac{1}{2}} = \left( \tau_{yT}^2 + \tau_{zT}^2 \frac{T^2}{R^2} \right)^{\frac{1}{2}} \quad (97c)$$

## 2.7 Summary

We have seen a variety of definitions of tunnelling time within the orthodox interpretation, both ‘intrinsic’ quantities defined without regard to the experimental apparatus (sections 2.2-2.3) and ‘experimental’ quantities defined with respect to a specific physical system (sections 2.4-2.6). Hauge and Støvneng (1989, section 1) outline three criteria that a definition must satisfy to be considered a valid definition of tunnelling time:

- The average duration of a physical process must be real.
- Due to the mutual exclusivity of transmission and reflection, reflection and transmission times must obey equation 36.
- Any proposed reflection and transmission times must obey any constraint that can be constructed from the dwell time.

The dwell time is not a contender for the definition of tunnelling time; although widely accepted within the literature, it does not distinguish between eventually reflected and eventually transmitted particles, and so is unable to answer the question of *when a particle with energy less than the barrier potential traverses the barrier region and is eventually transmitted, how much time did it, on average, spend in the barrier region?* It does however serve as an important consistency check for proposed definitions through equation 36.

The total phase times for transmission and reflection are well established but are *asymptotic* quantities which are only well-defined for completed scattering events. Extrapolating the spatial interval considered to the width of the barrier (the *extrapolated phase times*) introduces a contribution from the self-interference delay which cannot be neglected, meaning the quantity loses its physical meaning as the time spent in the barrier region.

The quantum clock model of Peres is nullified by the uncertainty principle; in the following sense, Peres himself concludes that achieving a clock with high time resolution increases the disturbance to the system under observation, and evolution of the system may even be halted by using a clock that is too precise, in a quantum analogue of Zeno's paradox. He comments that the time-dependent Schrödinger equation is an 'idealisation rooted in classical theory ... and should probably give way to a more complicated dynamical formalism'.

The Larmor clock also faces issues arising due to the uncertainty principle. The notion of a magnetic field *precisely* confined to a potential barrier is classical in nature, and Hauge and Støvneng (1989, section 4) construct an example in which the derived times do not obey equation 36. These problems can be solved by extending the spatial interval considered (similar to the asymptotic phase times, and hence called the 'asymptotic Larmor clock' (see e.g. Hauge and Støvneng 1989 (section 6)), but doing so yields the phase times which have been shown to be unsuitable for defining the tunnelling time through a potential barrier.

These conclusions lead one to question whether the notion of tunnelling time, or more specifically the mean transmission, reflection and dwell times, are well-defined within the orthodox interpretation. Some authors argue that such quantities are meaningless because they imply the notion of particle trajectories, the existence of which would violate the uncertainty principle. However, particle trajectories *are* a central feature within the de Broglie-Bohm interpretation, making it an ideal framework within which to study the subject of tunnelling times in quantum mechanics. To this, I now turn.

### 3 Tunnelling Times in the de Broglie-Bohm Interpretation

It is clear from the previous section that no definitive answer to the question ‘*How long does a particle take to tunnel through a quantum barrier*’ has been agreed upon within the orthodox interpretation of quantum mechanics. In contrast, the de Broglie-Bohm (dBB) interpretation yields a unique and well-defined prescription for defining tunnelling times. In section 3.1 I present the main ideas of this interpretation. Section 3.2 prescribes the natural definition of tunnelling time that arises within this interpretation; and in section 3.3, I discuss the results of numerical analysis of a Gaussian wave packet incident on a potential barrier within the de Broglie-Bohm interpretation. I conclude in section 3.4 with a discussion of the consequences of the conclusive answer offered by the de Broglie Bohm interpretation for verifying either the Copenhagen or pilot wave theories.

#### 3.1 de Broglie-Bohm Theory

The dBB theory is an interpretation of quantum mechanics built upon the following postulates (Holland 1993):

- P1 Individual physical systems comprise a wave propagating in space and time, and a point particle, the motion of which is guided by the wave.
- P2 The wave is mathematically described by  $\psi(t, \mathbf{y}) = Re^{iS/\hbar}$ ,  $R = R(t, \mathbf{y})$  is a real amplitude function,  $S = S(t, \mathbf{y})$  is a real phase function and  $\psi(t, \mathbf{y})$  satisfies the time-dependent Schrödinger equation.
- P3 The velocity of the particle is given by  $\mathbf{v} = \frac{1}{m}\nabla S$ . The particle motion is obtained by solving this equation along with the specification of the initial condition of the particle,  $\mathbf{y}(0)$ .
- P4 The probability of a particle *being* between points  $\mathbf{y}$  and  $\mathbf{y} + d\mathbf{y}$  at time  $t$  is given by:

$$|\psi(t, \mathbf{y})|^2 d^3y = R(t, \mathbf{y})^2 d^3y \quad (98)$$

The effect of this postulate is to extract from all possible motions of the particle those compatible with the initial distribution  $R(0, \mathbf{y})$ . Note how this differs from the orthodox interpretation in which  $|\psi(t, \mathbf{y})|^2$  is the probability density of finding a particle *upon measurement*.

Substituting in  $\psi = Re^{iS/\hbar}$  into the time-dependent Schrödinger equation yields:

$$\frac{\partial S}{\partial t} + \frac{(\nabla S)^2}{2m} - \frac{\hbar^2}{2m} \frac{\nabla^2 R}{R} + V = 0 \quad (99a)$$

$$\frac{\partial R^2}{\partial t} + \nabla \cdot \left( \frac{R^2 \nabla S}{m} \right) = 0 \quad (99b)$$

*Proof.*

$$i\hbar \frac{\partial \psi}{\partial t} = -\frac{\hbar^2}{2m} \nabla^2 \psi + V\psi \quad (100a)$$

$$i\hbar \left( \dot{R} + \frac{i}{\hbar} R\dot{S} \right) = -\frac{\hbar^2}{2m} \left( \nabla^2 R + \frac{2i}{\hbar} \nabla R \nabla S - \frac{1}{\hbar^2} R (\nabla S)^2 + \frac{i}{\hbar} R \nabla^2 S \right) + VR \quad (100b)$$

where the factor  $e^{iS/\hbar}$  has been cancelled on both sides. Isolating real and imaginary parts yields:

$$-R\dot{S} = -\frac{\hbar^2}{2m} \left( \nabla^2 R - \frac{R}{\hbar^2} (\nabla S)^2 \right) + VR \quad (100c)$$

$$\implies \frac{\partial S}{\partial t} + \frac{(\nabla S)^2}{2m} - \frac{\hbar^2}{2m} \frac{\nabla^2 R}{R} + V = 0 \quad (100d)$$

$$\hbar\dot{R} = -\frac{\hbar}{2m} (2\nabla R \nabla S + R \nabla^2 S) \quad (100e)$$

$$\implies \frac{\partial R^2}{\partial t} + \nabla \cdot \left( \frac{R^2 \nabla S}{m} \right) = 0 \quad (100f)$$

□

Note that (99b) can be written as:

$$\frac{\partial P(t, \mathbf{y})}{\partial t} + \nabla \cdot \mathbf{j}(t, \mathbf{y}) = 0 \quad (101)$$

where  $P$  is the probability density and  $\mathbf{j}$  is the 3-dimensional generalisation of the flux (35g), and hence takes the form of the continuity equation. Note also equation (99a) is a modified Hamilton-Jacobi equation, with additional term  $Q = -(\hbar^2/2m)\nabla^2 R/R$ , the ‘quantum potential energy’.

As in P3 one defines the vector field  $\mathbf{v} = \frac{1}{m}\nabla S$ , which defines at each point in space at each instant in time the tangent to the particle’s trajectory passing through that point. Given that the gradient  $\nabla S$  is orthogonal to level surfaces of  $S$ , the trajectories are orthogonal to surfaces  $S = \text{constant}$ , and are given by the solution of  $\dot{\mathbf{y}} = \frac{1}{m}\nabla S(t, \mathbf{y})$ , requiring specification of the initial condition  $\mathbf{y}_0$ . Hence the motion of the particle is completely deterministic once its initial position has been specified. Note that one does not have to specify an initial velocity  $\mathbf{v}_0$  as this is encoded in the initial wave  $\psi_0(\mathbf{y})$  and is calculated using P3. Note also the important fact that no two different trajectories with the same wave  $\psi(t, \mathbf{y})$  intersect. This is because at the point of intersection, both trajectories have the same velocity and position at the same point in time. As the motion of a particle is deterministic given the specification of an initial condition, the two trajectories will subsequently coincide for all times after the time of intersection. By time reversal invariance, the two trajectories must also have coincided for all antecedent times, a contradiction with our initial assumption.

From P3 it is clear that an ensemble of possible motions associated with the same wave is generated by varying the initial condition  $\mathbf{y}_0$ . Once specified, the laws governing the evolution of a physical system are entirely deterministic. The probabilistic nature of quantum mechanics, familiar from experiments such as the double-slit experiment, is recovered from the fact that giving a particle a precisely defined initial condition is empirically unrealisable. Hence given an ensemble of identical physical systems (a wave and point particle), it is the uncertainty of the initial position of the particles, as encoded in P4, that gives rise to the probabilistic nature of quantum mechanics.

### 3.2 A Natural Definition of Tunnelling Time

The notion of a particle trajectory in the dBB theory leads one to a natural definition of reflection and transmission times. For a particle with initial condition (again restricting to the one-dimensional case)  $y = y_0$  at  $t = 0$ , the time spent in the region  $y_1 \leq y \leq y_2$  is given by:

$$t(y_0; y_1, y_2) = \int_0^\infty dt \Theta(y(t, y_0) - y_1) \Theta(y_2 - y(t, y_0)) \quad (102)$$

where  $y(t, y_0)$  denotes the position at time  $t$  of a particle with initial condition  $y = y_0$  at  $t = 0$  and  $\Theta$  is the Heaviside step function. Such an expression is classical in nature; it holds identically in classical mechanics, where  $y(t, y_0)$  is the particle position obtained from solving its equation of motion. This definition is intuitively clear:  $\Theta(y(t, y_0) - y_1)$  has support for particle positions  $> y_1$ , and  $\Theta(y_2 - y(t, y_0))$  has support for particle positions  $< y_2$ . When a position satisfies both of these conditions, the particle resides within the interval of interest  $(y_1, y_2)$  and thus (102) integrates 1 over the interval of time the particle is between  $y_1$  and  $y_2$ .

For empirical purposes, the precise specification of the particle’s initial condition is not possible. For an ensemble of identical systems, one can use P4 at  $t = 0$  to state the probability distribution of initial positions, and hence define the *mean dwell time*:

$$\tau_D(y_1, y_2) = \langle t(y_0; y_1, y_2) \rangle := \int_{-\infty}^\infty dy_0 |\psi(0, y_0)|^2 t(y_0; y_1, y_2) \quad (103a)$$

$$\stackrel{(102)}{=} \int_{-\infty}^\infty dy_0 |\psi(0, y_0)|^2 \int_0^\infty dt \Theta(y(t, y_0) - y_1) \Theta(y_2 - y(t, y_0)) \quad (103b)$$

$$= \int_{-\infty}^{\infty} dy_0 |\psi(0, y_0)|^2 \int_0^{\infty} dt \int_{-\infty}^{\infty} dy \Theta(y - y_1) \Theta(y_2 - y) \delta(y - y(t, y_0)) \quad (103c)$$

$$= \int_0^{\infty} dt \int_{y_1}^{y_2} dy \int_{-\infty}^{\infty} dy_0 |\psi(0, y_0)|^2 \delta(y - y(t, y_0)) \quad (103d)$$

$$= \int_0^{\infty} dt \int_{y_1}^{y_2} dy |\psi(t, y)|^2 \quad (103e)$$

where  $|\psi(t, y)|^2 = \langle \delta(y - y(t, y_0)) \rangle$  (cf. Leavens and Aers 1990 (6.18)). Leavens and Aers (1989 pp. 1204) argue this is identical to the dwell time derived previously (34).

One can use the fact that particle trajectories do not intersect each other to define a starting point  $y_0^c$  such that only trajectories  $y(t, y_0)$  with  $y_0 > y_0^c$  are ultimately transmitted, and trajectories with  $y_0 < y_0^c$  are ultimately reflected (Figure 7).  $y_0^c$  is defined by:

$$\int_{y_0^c}^{\infty} dy_0 |\psi(0, y_0)|^2 = |T|^2 \quad (104)$$

This definition is intuitively clear - the left hand side is the probability a particle starts in a region that guarantees it will be ultimately transmitted; thanks to the determinism of the theory, this is equal to the transmission probability.

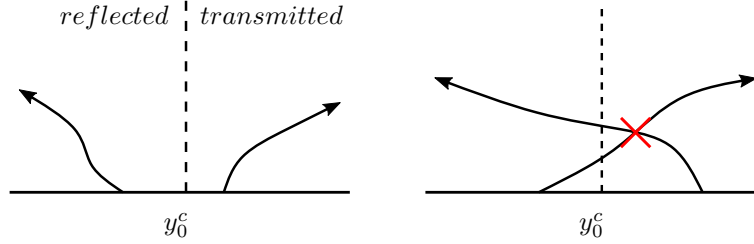


Figure 7:  $y_0^c$  separates reflected and transmitted trajectories.

Thanks to the determinism of the theory and the prediction that trajectories may not intersect, for an initial wave packet to the left of the barrier whose centroid coincides with the reflection-transmission bifurcation point, those particles in the ‘front-half’ of the wave function will be ultimately transmitted, while those in the ‘back-half’ will be ultimately reflected.

Subsequently one can calculate the mean transmission and reflection times, uniquely given by:

$$\tau_T(y_1, y_2) = \frac{\langle (t(y_0; y_1, y_2) \Theta(y_0 - y_0^c)) \rangle}{\langle \Theta(y_0 - y_0^c) \rangle} \quad (105)$$

$$\tau_R(y_1, y_2) = \frac{\langle (t(y_0; y_1, y_2) \Theta(y_0^c - y_0)) \rangle}{\langle \Theta(y_0^c - y_0) \rangle}. \quad (106)$$

where  $|T|^2 = \langle \Theta(y_0 - y_0^c) \rangle$  and  $|R|^2 = \langle \Theta(y_0^c - y_0) \rangle$ . These are real-valued, non-negative quantities obeying the consistency condition (36):

$$|T|^2 \tau_T(y_1, y_2) + |R|^2 \tau_R(y_1, y_2) = \langle (t(y_0; y_1, y_2) \Theta(y_0 - y_0^c)) \rangle + \langle (t(y_0; y_1, y_2) \Theta(y_0^c - y_0)) \rangle \quad (107a)$$

$$= \langle (t(y_0; y_1, y_2) (\Theta(y_0 - y_0^c) + \Theta(y_0^c - y_0))) \rangle \quad (107b)$$

$$= \langle t(y_0; y_1, y_2) \rangle = \tau_D \quad (107c)$$

The probability distributions of the transmission and reflection times,  $P_T$  and  $P_R$ , are also of interest. These are defined by:

$$\tau_T(y_1, y_2) = \int_0^{\infty} dt P_T(t(y_1, y_2)) t, \quad \tau_R(y_1, y_2) = \int_0^{\infty} dt P_R(t(y_1, y_2)) t; \quad (108)$$

and hence are given by

$$P_T(t(y_1, y_2)) := \frac{\langle (\Theta(y_0 - y_0^c)) \delta[t(y_1, y_2) - t(y_0; y_1, y_2)] \rangle}{\langle \Theta(y_0 - y_0^c) \rangle} \quad (109a)$$

$$P_R(t(y_1, y_2)) := \frac{\langle (\Theta(y_0^c - y_0)) \delta[t(y_1, y_2) - t(y_0; y_1, y_2)] \rangle}{\langle \Theta(y_0^c - y_0) \rangle}. \quad (109b)$$

### 3.3 Numerical Example

In this section I discuss the results of two complementary numerical analyses of a Gaussian wave packet incident on a potential barrier. The first analysis (section 3.3.2) was performed by the author using the implicit second-order Crank-Nicolson method. The analysis yields approximations to the time-evolution of the wave function and the large-scale behaviour of particle trajectories (relative to the width of the barrier). The second analysis (section 3.3.3) was originally presented by Leavens and Aers (1990, section 6.4.3) using the fourth order de Raedt symmetrised product formula method, and yields approximations to the small-scale behaviour of particle trajectories and probability distributions as described in section 3.2.

#### 3.3.1 Parameters

Consider tunnelling through a barrier with boundaries shifted to  $[0, d]$  and a particle with initial Gaussian wave function:

$$\psi(t=0, y) = \frac{1}{(2\pi(\Delta y)^2)^{\frac{1}{4}}} \exp\left(-\left(\frac{(y-y_0)^2}{2\Delta y}\right)^2 + ik_0 y\right) \quad (110)$$

where  $y_0$  is the centroid of  $|\psi(0, y)|^2$  and  $k_0$  is the centroid of  $|\phi(k)|^2$ , the Fourier transform of the wave function in momentum space. This is a minimum-uncertainty wave function and hence the uncertainties of its position and momentum satisfy  $\Delta y \Delta k = \frac{1}{2}$  (with  $\hbar = 1$ ).  $y_0$  is chosen such that the wave function is sufficiently far to the left of the barrier region  $0 \leq y \leq d$  such that the initial probability density  $|\psi(0, y)|^2$  is negligible for  $y \geq 0$ . The time evolution of the wave function is dictated by the time-dependent Schrödinger equation:

$$i\hbar \frac{\partial}{\partial t} \psi(t, y) = H(t, y) \psi(t, y) \quad (111)$$

with the Hamiltonian given by

$$H(y) = -\frac{\hbar^2}{2m} \frac{\partial^2}{\partial y^2} + V_0 \Theta(y) \Theta(d - y) \quad (112)$$

The analyses presented consider a barrier with height  $V_0 = 10eV$  and variable widths. The incident particle has energy  $E_0 = V_0/2$ , variable momenta uncertainties  $\Delta k$  and trajectory starting points  $y(t=0)$  near the transmission-reflection bifurcation point  $y_0^c$ .

#### 3.3.2 Crank-Nicolson Method

The problem has first been solved numerically by the author (converting to atomic units  $\hbar = m = 1$ ) using the Crank-Nicolson method as presented in Dubeibe (2010, section 2) in Mathematica 12.0: A formal solution to (111) can be expressed in terms of the time-evolution operator as  $\psi(t, y) = U(t, 0) \psi(0, y) = e^{-iHt} \psi(0, y)$ . For evolution over one time step  $\Delta t$ ,  $U(t + \Delta t, t)$  can be represented in Cayley form (accurate to second-order in  $\Delta t$ ):

$$U(t + \Delta t, t) = \frac{1 - \frac{i\Delta t}{2} H(t, y)}{1 + \frac{i\Delta t}{2} H(t, y)} \quad (113)$$

from which one deduces the wave function at times  $t, t + \Delta t$  obeys:

$$\left(1 + \frac{i\Delta t}{2}H(t, y)\right)\psi(t + \Delta t, y) = \left(1 - \frac{i\Delta t}{2}H(t, y)\right)\psi(t, y) \quad (114)$$

Discretising the wave function domain to a grid of length  $t_{max}, y_{max}$  with subintervals  $\Delta t, \Delta y$ :

$$\left(1 \pm \frac{i\Delta t}{2}H\right)\psi_j^n \approx \psi_j^n \pm \frac{i\Delta t}{2}\left(-\frac{\psi_{j+1}^n - 2\psi_j^n + \psi_{j-1}^n}{2\Delta y^2} + V_j^n\psi_j^n\right) \quad (115)$$

where  $\psi_j^n = \psi(t_n, y_j), V_j^n = V(t_n, y_j)$  and the second order spatial partial derivative in (112) has been approximated by the Crank-Nicolson approximation. By substitution of (115) in to (114),  $\vec{\psi}^{t+\Delta t} = (\psi_1^{t+\Delta t}, \dots, \psi_{y_{max}}^{t+\Delta t})$  can be obtained by multiplication of  $\vec{\psi}^t = (\psi_1^t, \dots, \psi_{y_{max}}^t)$  by suitable tridiagonal matrices  $D_1, D_2$ :

$$\vec{\psi}^{t+\Delta t} = D_2^{-1}D_1\vec{\psi}^t = \left(1 + \frac{i\Delta t}{2}H\right)^{-1}\left(1 - \frac{i\Delta t}{2}H\right)\vec{\psi}^t \quad (116)$$

the form of which can be easily calculated using (115).

In this analysis, the wave function is constrained to a line of length  $y_{max} = 400a_0$  ( $210\text{\AA}$ ) discretised into a grid of spacing  $\Delta y = 2a_0$  ( $1.1\text{\AA}$ ), and evolves over a time period  $t_{max} = 600au$  ( $1.44 \times 10^{-14}s$ ) discretised into a grid of spacing  $\Delta t = 0.6au$  ( $1.44 \times 10^{-17}s$ ). The location of the centroid  $y_0$  is  $-175a_0$  ( $-92.5\text{\AA}$ ) and in this example,  $\Delta k = 0.021a_0^{-1}$  ( $0.04 \text{\AA}^{-1}$ ). The barrier has width  $d = 19a_0$  ( $10\text{\AA}$ ). (for unit conversions see e.g. Weinhold and Landis 2012 (Appendix E)).

First I present the numerical simulation of the time evolution of the wave function. The real component of the wave function evolves in time as shown in Figure 8. The wave function approaches the barrier and begins to appreciably interact with it at a time of approximately  $4.4 \times 10^{-15}s$ . The presence of the potential barrier causes a significant disturbance to the wave function's free evolution. The majority of the wave is reflected by the barrier, with a small component being transmitted past the barrier into the classically forbidden region.

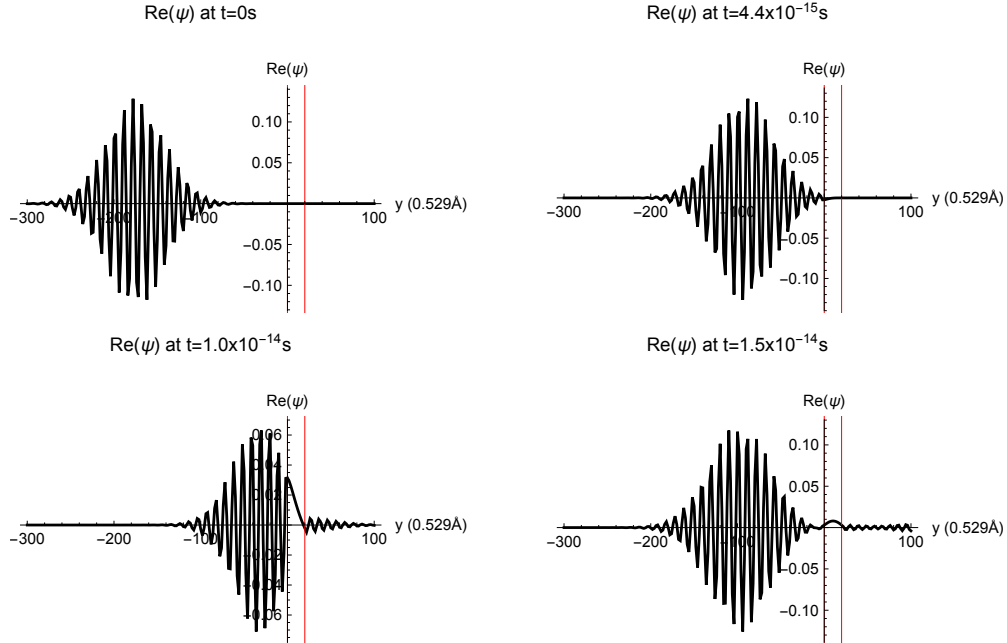


Figure 8: Time evolution of the real part of the Gaussian wave function. The location of the potential barrier is indicated by the vertical red lines.

I now present the large-scale trajectories of particles incident on the potential barrier. Figure 9 shows the time evolution of particle trajectories dependent on the initial position  $y(t = 0)$ . The trajectories were

obtained by calculating the particle velocity (cf. P3) at each grid location,  $v(t_n, y_j)$ . For each trajectory, the particle location was incremented by the  $\Delta t \times v(t_n, y_j)$  at each time-step  $n = \{0, 1, \dots, t_{max}/\Delta t\}$  where  $y_j$  denotes the particle's location at time  $t_n$ . One observes that the particle trajectories do not intersect, as predicted by the theory. The trajectory beginning at  $-20a_0$  achieves tunnelling. Trajectories from  $-80a_0$  to  $-40a_0$  successfully penetrate the barrier, but oscillate within it before eventually being reflected. Particles with initial positions less than this traverse towards the barrier but are ultimately reflected without achieving barrier penetration. The results are qualitatively similar to those of Leavens and Aers (1990) (Figure 10) and are very similar to those of Dewdney and Hiley (1982, section 4).

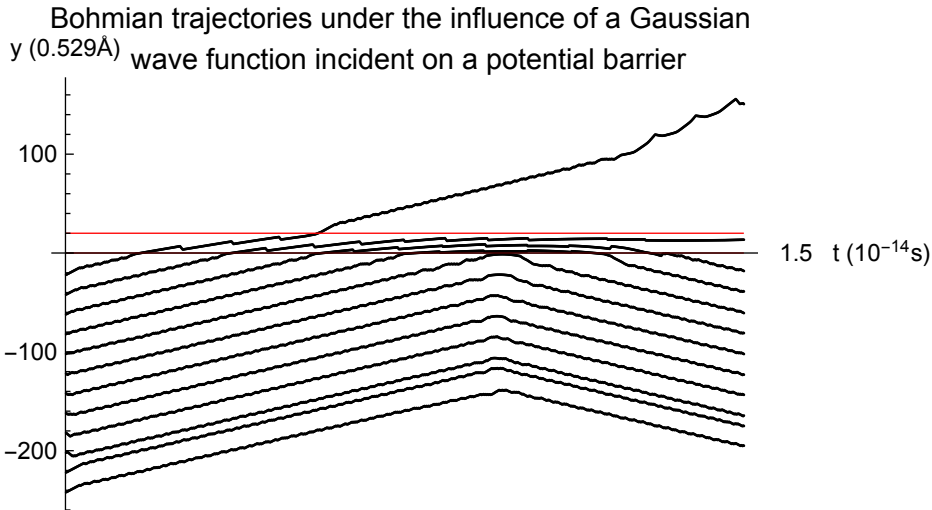


Figure 9: Large scale trajectories of particles incident on a potential barrier with parameters given in section 3.3.1.

### 3.3.3 de-Raedt Method

The problem has been solved by Leavens and Aers (1990, section 6.4.3). This analysis focuses on the behaviour of particle trajectories near the reflection-transmission bifurcation point so offers insight in to the physical consequences of the theoretical predictions made in section 3.2. It also offers a comparison with the Larmor clock times in section 2.6, demonstrating the starkly different predictions made by the two theories. The de-Raedt method directly addresses some of the computational issues of the Crank-Nicolson method of the previous section, allowing for more detailed (small scale) analysis and making it the natural choice of higher-order analysis to report. The de-Raedt symmetrised product formula method decomposes the Hamiltonian into a sum of simpler operators,  $H = \sum_q H_q$ , that are sufficiently simple so that they can be diagonalised easily. The time evolution operator is then approximated by ordered products of exponentials of the form  $e^{-iH_q t}$  (de Raedt 1987 section 1).

Figure 10a shows the Bohm trajectories for a Gaussian wave function incident on a barrier of height  $V_0 = 10eV$  and width  $d = 5\text{\AA}$ . The parameters of the wave packet are:  $\Delta k = 0.04\text{\AA}^{-1}$ ,  $y_0 = -71.80\text{\AA}$  (dashed lines) and  $\Delta k = 0.08\text{\AA}^{-1}$ ,  $y_0 = -35.58\text{\AA}$  (solid lines). One clearly observes particles in the ‘front half’ of the wave packet being transmitted and those in the ‘back half’ being reflected, as discussed in section 3.2. The authors also identify the factor of  $\sim 2$  difference in time scales for motion within the barrier, with lower  $\Delta k$  corresponding to higher duration. Figure 10b shows the dependence of transmission time on the energy  $E_0$  of a Gaussian wave packet incident on a barrier of height  $V_0 = 10eV$ , width  $d = 3\text{\AA}$ . The circular and triangular data points denote the Bohm trajectory results for  $\Delta k = 0.04\text{\AA}^{-1}$  and  $0.08\text{\AA}^{-1}$  respectively, with corresponding Larmor clock results shown by the solid and dashed lines. Note the two sets of results significantly differ for energies below the barrier height, but coincide well once the incident particle energy is well above the barrier height.

Figure 10c shows the dependence of tunnelling time on the width of the rectangular barrier of height

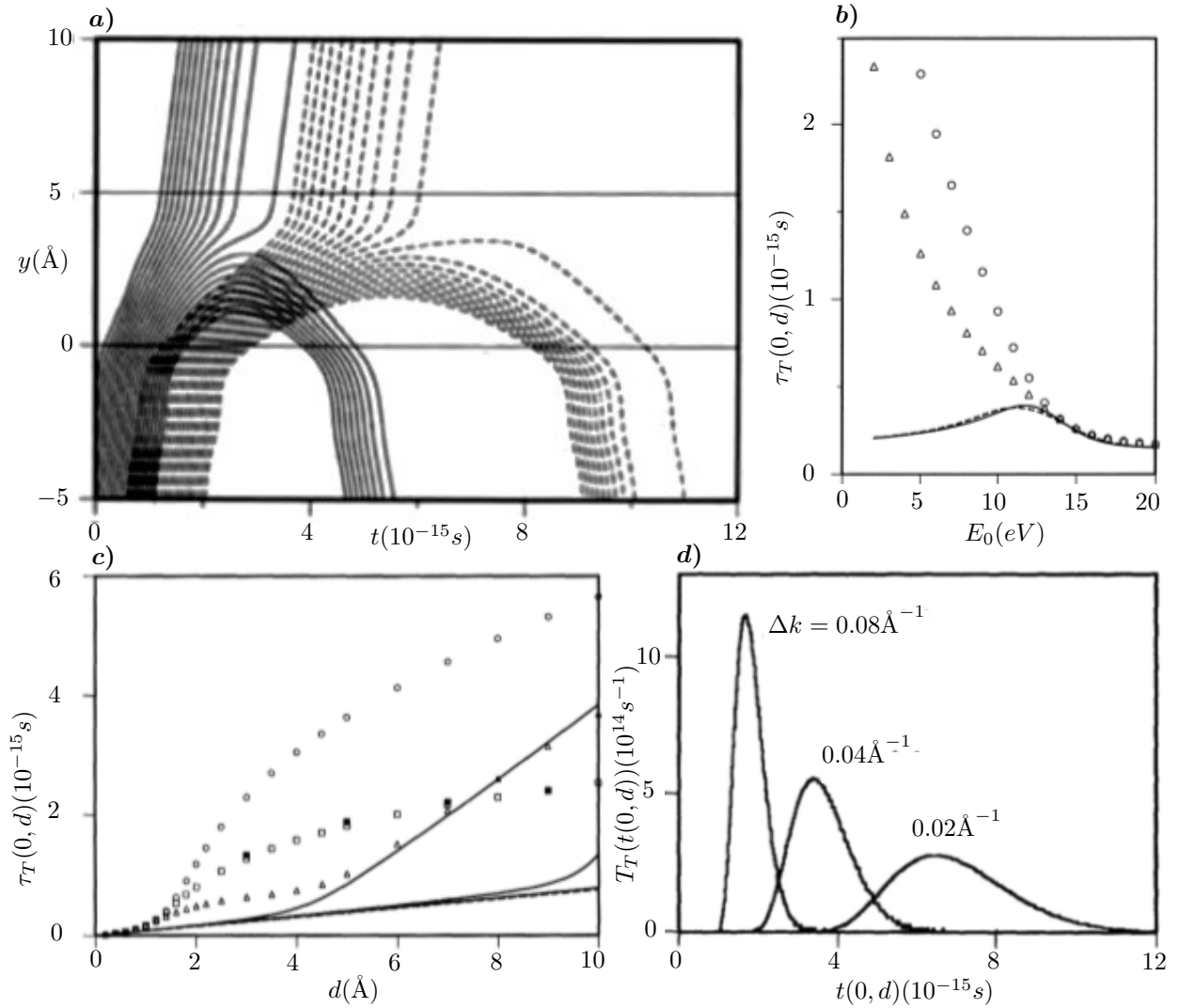


Figure 10: Quantum tunnelling results of Leavens and Aers (1990 pp. 117-120) using the de-Raedt method.

$V_0 = 10eV$  and incident energy  $E_0 = 5eV$ . The circular, square and triangular data points denote the Bohm trajectory results for  $\Delta k = 0.04\text{\AA}^{-1}$ ,  $0.08\text{\AA}^{-1}$  and  $0.16\text{\AA}^{-1}$  respectively, with corresponding Larmor clock results shown by the lower, middle and upper solid lines respectively. The dashed line shows the free particle result ( $V_0 = 0$ ). Figure 10d expound the observation made of Figure 10a, showing the transmission time distributions for a barrier of height  $V_0 = 10eV$  and width  $d = 2.0\text{\AA}$  and  $5.0\text{\AA}$  respectively. One observes wave packets with higher  $\Delta k$  have low-variance distributions with low modal values, compared to lower  $\Delta k$  wave packets with high-variance distributions with higher modal values. All distributions have positive skew: this is a consequence of the fact that transmitted trajectories near the transmission-reflection bifurcation point spend a long time inside the barrier.

### 3.4 A Crucial Experiment?

The de Broglie-Bohm and orthodox interpretations are predicted to be observationally equivalent; more precisely, the two theories should always make identical predictions of the outcome of an experiment measuring quantities that are well defined within both interpretations. It is clear from the discussions in the preceding sections that the de Broglie-Bohm interpretation offers a well-defined and unambiguous prescription for cal-

culating tunnelling times, whereas the orthodox interpretation yields no unanimous answer and raises the question of whether the tunnelling times are well-defined within the orthodox viewpoint.

Can the divergence in the meaningfulness of tunnelling times between the two theories be exploited by an experiment to verify either interpretation? The orthodox interpretation, yielding no unambiguous predictions, can neither be supported or refuted, whereas the de Broglie-Bohm interpretation can be falsified if its theoretical predictions do not align with experiment. Cushing (1995, section 3) proposes an experimental set-up to test the predictions of the dBB theory: A state-preparation device releases a particle incident on a potential barrier, the reflection or transmission of which is detected by two detectors either side of the barrier. The dwell, reflection and transmission times could then be calculated:

$$\tau_D = \frac{1}{N} \sum_{j=1}^N \tau_j \quad \tau_R = \frac{1}{N_R} \sum_{\{N_R\}} \tau_j \quad \tau_T = \frac{1}{N_T} \sum_{\{N_T\}} \tau_j, \quad (117)$$

and compared with theoretical predictions. Other authors e.g. Field (2020, section 3.4) argue against this: despite the de Broglie-Bohm theory predicting well-defined particle trajectories, the behaviour of which upon interaction with the barrier is pre-determined, it is not possible to use a measurement device to isolate particles in reflected and transmitted channels without disturbing the underlying dynamics. Hence an experimental observer only has access to the indeterministic behaviour of the wave function, so that any observations should be identical to those predicted within the orthodox viewpoint. Even if an experimentally derived quantity was identified with the tunnelling time in the de Broglie-Bohm interpretation, it may not be accepted by proponents of orthodoxy, especially if they consider the notions of transmission and reflection times to be meaningless.

## 4 Conclusion

We have seen in sections 2 and 3 that there are two consistent approaches to the question *how long does a quantum particle take to tunnel through a classically forbidden potential barrier?*

Within the orthodox interpretation, the concept of tunnelling time is ambiguous and a universally agreed-upon answer is not (yet) available. Many answers have been posed, of which section 2 is a small selection. In particular, the phase times (section 2.2) and dwell time (section 2.3) offer well-established quantities, but are manifestly unable to precisely answer the question at hand. However they serve as useful consistency checks for alternative definitions of tunnelling time, so are clearly of academic importance. The quantum clocks (sections 2.4-2.5) and Larmor clock (section 2.6) both offer methods of measuring time, but both are intrinsically linked to a physical system; the former requires the construction of a quantum clock (a physical system itself) being coupled to a physical system of interest, and the latter only defined for a quantum potential containing a magnetic field. As such, both clocks suffer from consequences of the Heisenberg uncertainty principle, and neither arise from purely theoretical (experimentally agnostic) considerations, which would be universally applicable and most satisfying. The issues faced by the orthodox interpretation stem from the fact that time is not a dynamical variable, and hence the measurement of time is in fact the measurement of a dynamical variable that resembles the time coordinate of space-time. Even if such a dynamical variable were to exist for a given physical system, to claim that it answers the question at hand would (in the author's opinion) be ill-founded unless its validity extends to all physical systems, including those living beyond one dimension as have been considered in this essay.

The de Broglie-Bohm interpretation is well suited to study the subject of tunnelling times. The notion of a deterministic particle trajectory (section 3.1) immediately resolves the issues surrounding the meaningfulness of tunnelling times that frustrate the orthodox viewpoint. As such, there exists a clear, unambiguous and well defined definition of tunnelling time, inherited from classical mechanics (section 3.2), which yields theoretical predictions (section 3.3), the testability of which is not yet clear. Clearly, this definition alleviates concerns raised within the orthodox viewpoint, that a most satisfying answer to the question at hand is purely theoretical, and agnostic to the experiment it is applied to. However while the question of whether tunnelling times are a meaningful quantity within the orthodox viewpoint remains contentious, and without an *experimentum crucis* to verify the de Broglie Bohm interpretation (section 3.4), the predictions remain a quirk of the theory to the majority of the scientific community. If the notion of tunnelling times can be proven to be well-established within the orthodox viewpoint, it would strengthen the answers posed by both interpretations.

Further research in this topic can take a variety of directions. Within the orthodox interpretation, proof of the meaningfulness of tunnelling times would motivate the need for further study and perhaps guide the scientific community towards a consistent and conclusive answer. Disproof of the statement would suggest either that time is treated unsatisfactorily within quantum mechanics, or that the question at hand is ill-founded. Within the de-Broglie Bohm interpretation, further research, both theoretical and technical, is required to establish whether an *experimentum crucis* can be conducted to break the empirical equivalence of the two interpretations. There is however another more radical avenue of research; ultimately it seems dissatisfying that quantum mechanics is unable to provide a conclusive answer to a seemingly innocuous question asked of one of its most profound predictions: quantum tunnelling. Treating time on a less fundamental footing than other quantities appears to be the root of the problems faced when approaching this subject. Perhaps approaching the problem via an alternative dynamical formalism, or within a more fundamental theory such as quantum field theory, would yield more consistent answers. I hope that through further research in the foundations of quantum physics, progress can be made to offer a more conclusive answer to this question.

## 5 Acknowledgements

I am extremely grateful to J. N. Butterfield for his guidance, advice and enthusiasm, G. Field for her valuable discussions and early access to her paper, and B. Roberts for his helpful comments.

## References

- [1] Büttiker, M. (1983), Larmor precession and the traversal time for tunnelling, *Physical Review B* **27**, 6178-6188
- [2] Butterfield, J.N. (2012), On time in quantum physics, in *A Companion to the Philosophy of Time*, Dyke, H., Bardon, A., Wiley
- [3] Cushing, J.T. (1995), Quantum tunneling times: A crucial test for the causal program?, *Foundations of Physics* **25**, 269-280
- [4] Dewdney, C., Hiley, B.J. (1982), A quantum potential description of one-dimensional time-dependent scattering from square barriers and square wells, *Foundations of Physics* **12**, 27-48
- [5] Dubeibe, F.L. (2010), Solving the time-dependent Schrödinger equation with absorbing boundary conditions and source terms in Mathematica 6.0, *International Journal of Modern Physics C*, 1-14
- [6] Field, G. (2020), Quantum tunneling times: No crucial test for the causal program, Cambridge University
- [7] Goldstein, H., Safko, J.L., Poole, C.P. (2002), *Classical Mechanics* (3rd ed.), Addison-Wesley
- [8] Hauge, E. and Støvneng J. (1989), Tunneling times: a critical review, *Reviews of Modern Physics* **61**, 917–936
- [9] Hilgevoord, J. (2002), Time in quantum mechanics, *American Journal of Physics* **70**, 301-306
- [10] Holland, P.R. (1993), *The Quantum Theory of Motion*, Cambridge University Press
- [11] Leavens, C.R. (1990), Traversal times for rectangular barriers within Bohm’s causal interpretation of quantum mechanics, *Solid State Communications* **76**, 253-261
- [12] Leavens, C.R. (1996), The “tunneling-time problem” for electrons, in *Bohmian Mechanics and Quantum Theory: An Appraisal*, Cushing, J.T., Fine, A., Goldstein, S. (eds), Springer
- [13] Leavens, C.R., Aers, G.C. (1989), Dwell time and phase times for transmission and reflection, *Physical Review B* **39**, 1202-1206
- [14] Leavens, C.R., Aers, G.C. (1990), Tunnelling times for one-dimensional barriers, in *Scanning Tunnelling Microscopy and Related Methods*, Behm R.J., Garcia N., Rohrer H. (eds), Springer
- [15] Peres, A. (1980), Measurement of time by quantum clocks, *American Journal of Physics* **48**, 552–557
- [16] de Raedt, H. (1987), Product formula algorithms for solving the time dependent Schrödinger equation, *Computational Physics Reports* **7**, 1-72
- [17] Rybachenko, V.F. (1967), Time of penetration of a particle through a potential barrier, *Soviet Journal of Nuclear Physics* **5**, 635-639
- [18] Sakurai, J.J., Napolitano, J.J. (2017), *Modern Quantum Mechanics*, Cambridge University Press
- [19] Weinhold, F., Landis, C.R. (2012), *Discovering Chemistry with Natural Bond Orbitals* (1st ed.), Wiley